Gravitational wave results from LIGO and Virgo

Jo van den Brand, Nikhef and VU University Amsterdam, jo@nikhef.nl

High Energy Phenomena in Relativistic Outflows, HEPRO VII, Barcelona, July 12, 2019

LSC LIGO Scientific Collaboration

Advanced Virgo

LIGO and Virgo

Observe together as a Network of GW detectors. LVC have integrated their data analysis

LIGO and Virgo have coordinated data taking and analysis, and release joint publications
LIGO and Virgo work under an MOU already for more than a decade
KAGRA in Japan is expected to join in 2019

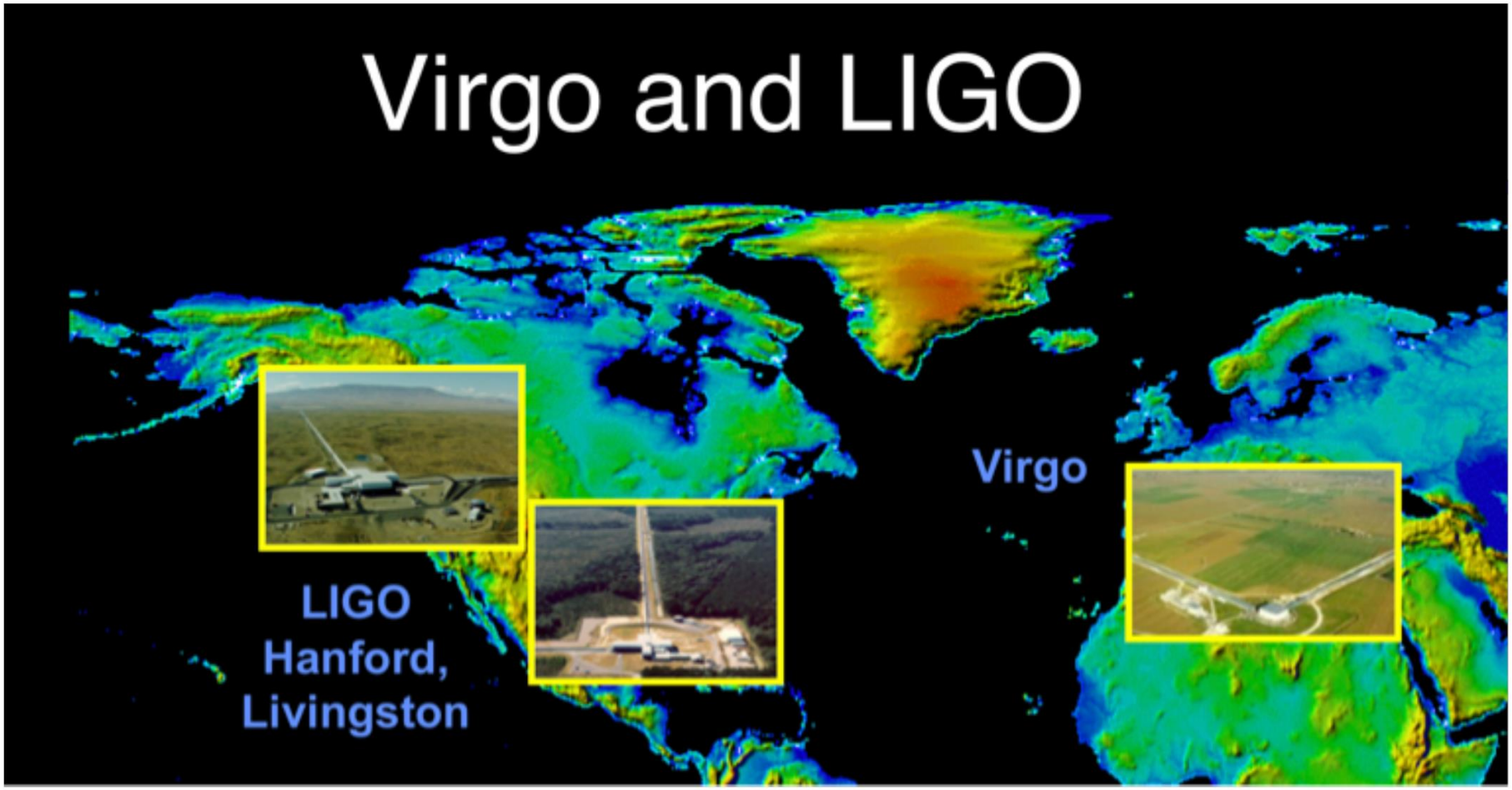

Virgo Collaboration has invested in Advanced Virgo

Virgo is a European collaboration with about 400 members from about 80 institutes

Advanced Virgo (AdV) and AdV+: upgrades of the Virgo interferometric detector

Participation by scientists from France, Italy, Belgium, The Netherlands, Poland, Hungary, Spain, Germany

- Institutes in Virgo Steering Committee
  - APC Paris
  - ARTEMIS Nice
  - IFAE Barcelona
  - INFN Firenze-Urbino
  - INFN Genova
  - INFN Napoli
  - INFN Perugia
  - INFN Pisa
  - INFN Roma La Sapienza
  - INFN Roma Tor Vergata
  - INFN Trento-Padova
  - LAL Orsay – ESPCI Paris
  - LAPP Annecy
  - LKB Paris
  - LMA Lyon
  - Maastricht University
  - Nikhef Amsterdam
  - POLGRAW(Poland)
  - RADBOUD Uni. Nijmegen
  - RMKI Budapest
  - UCLouvain, ULiege
  - Univ. of Barcelona
  - University of Sannio
  - Univ. of Valencia
  - University of Jena

Advanced Virgo project has been formally completed on July 31, 2017

Part of the international network of 2nd generation detectors

Joined the O2 run on August 1, 2017

LIGO and Virgo running of O3

8 European countries

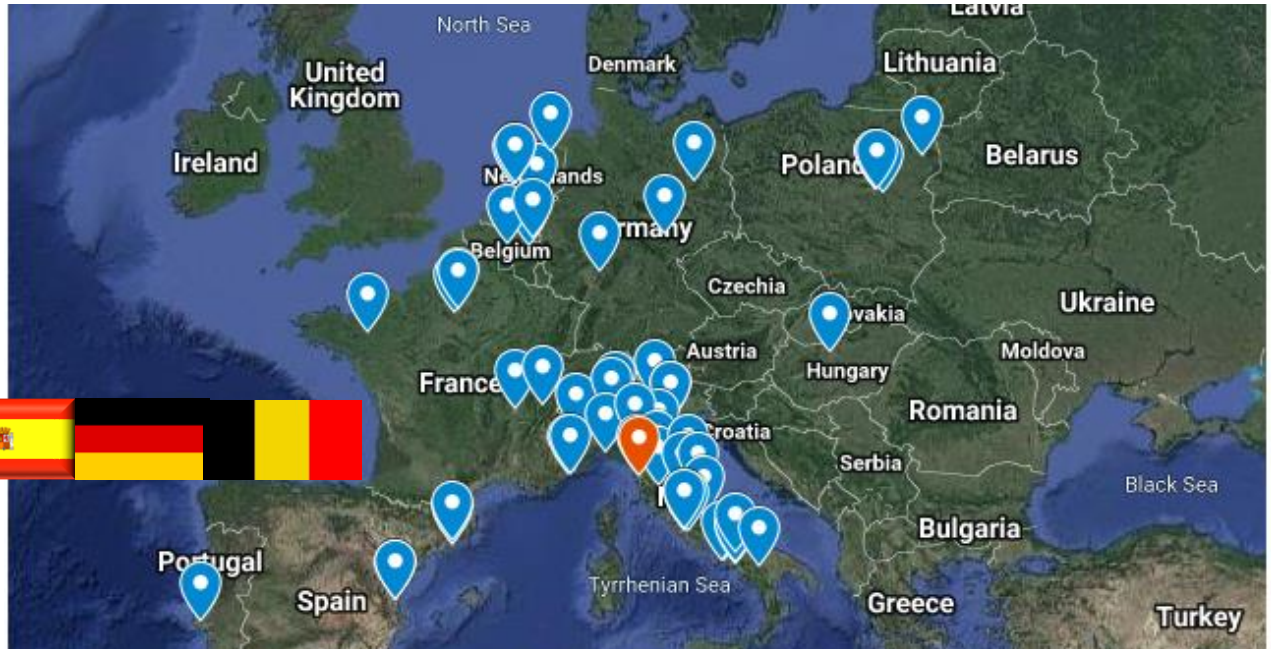

IFAE and University of Barcelona joined Virgo last year

New groups strengthen Virgo in areas as Computing and Stray Light Mitigation

2018: IFAE, UBarcelona, ULiege and UCLouvain joined the Virgo Collaboration

2019: USannio/UniSA, Jena University, Maastricht University

Groups from UTorino, USardinia, joined Virgo indirectly

ULBrussels, UAntwerp, UGhent, UUtrecht, KULeuven, KIT, … in discussion

LIGO and Virgo completed observation runs O1 and O2

Gravitational waves were discovered with the LIGO detectors on September 14, 2015. In total 3 events were detected in O1. The Advanced Virgo detector joined at the end of O2

We knew about only 2 events in O2 at the time Virgo turned on

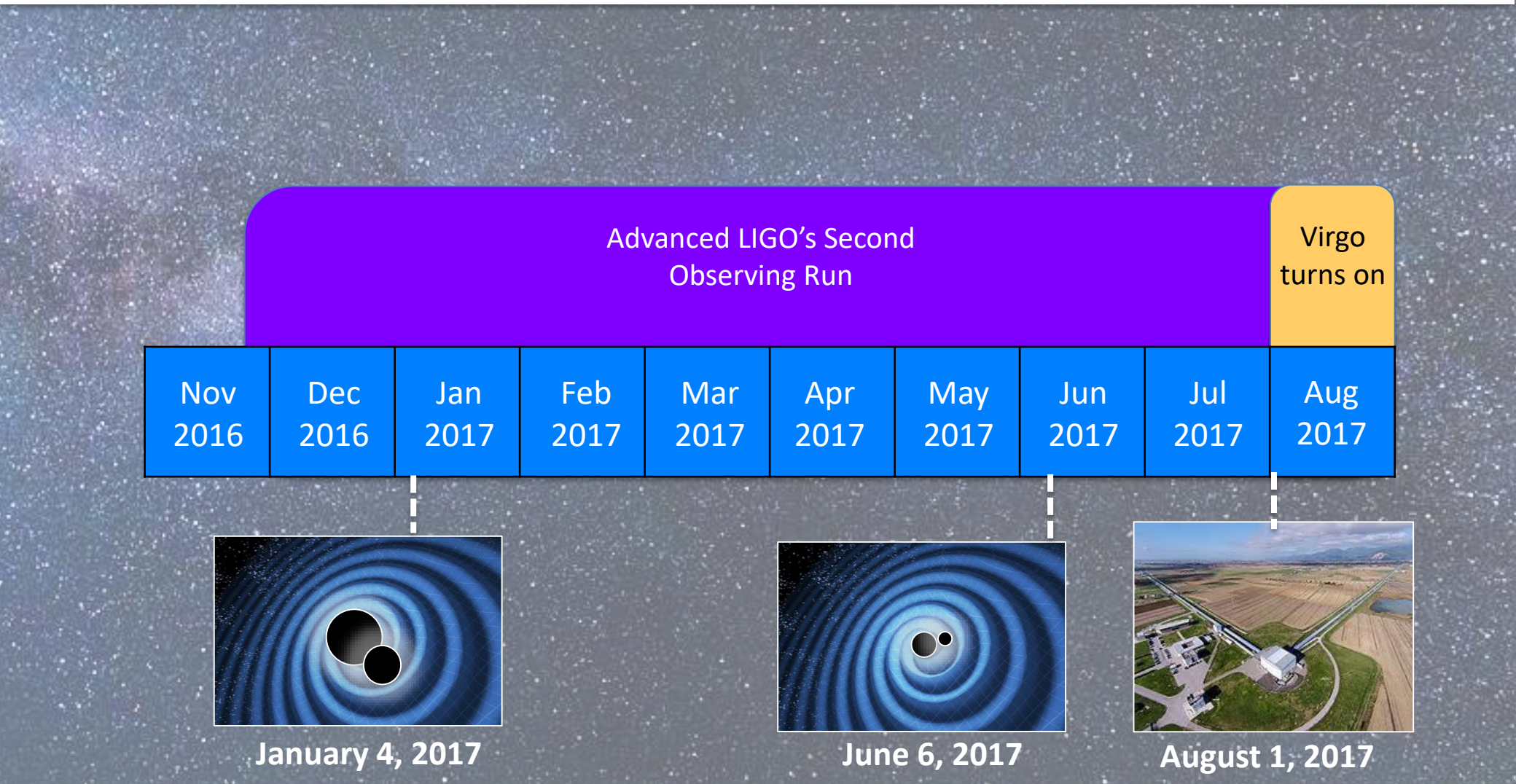

Scientific achievements: properties of binary systems

"GWTC-1: A Gravitational-Wave Transient Catalog of Compact Binary Mergers Observed by LIGO and Virgo during the First and Second Observing Runs", LIGO Virgo Collaboration, arXiv:1811.12907

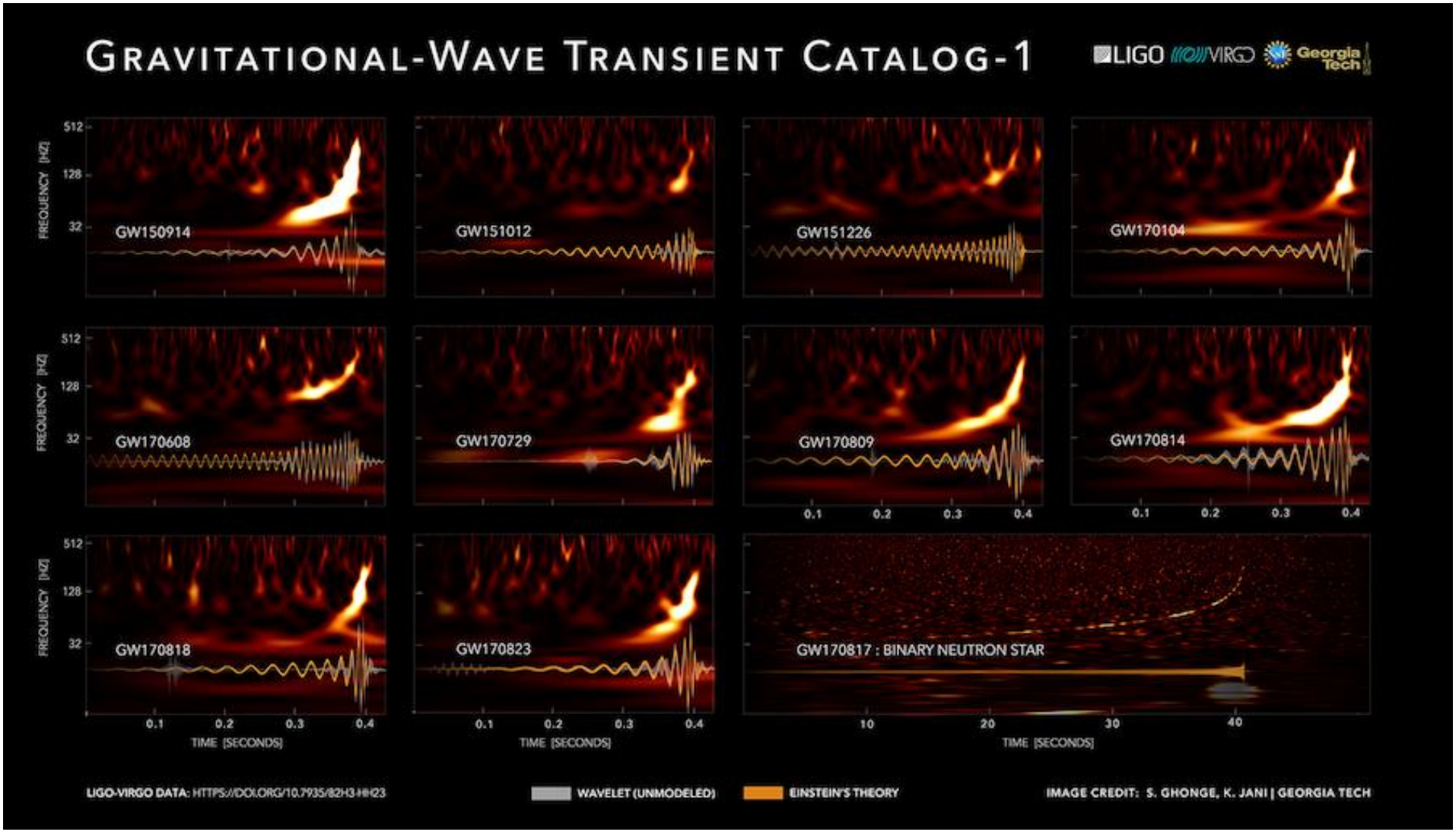

Table of O1 and O2 triggers with source properties

See arXiv:1811.12907

Event	$m_1/M_\odot$	$m_2/M_\odot$	$\mathcal{M}/M_\odot$	$\chi_{\rm eff}$	$M_{\rm f}/M_\odot$	$a_{\rm f}$	$E_{\rm rad}/(M_\odot c^2)$	$\ell_{\rm peak}/({\rm erg\ s^{-1}})$	$D_{\rm L}/{\rm Mpc}$	z	$\Delta\Omega/{\rm deg}^2$
GW150914	$35.6^{+4.8}_{-3.0}$	$30.6^{+3.0}_{-4.4}$	$28.6^{+1.6}_{-1.5}$	$-0.01^{+0.12}_{-0.13}$	$63.1^{+3.3}_{-3.0}$	$0.69^{+0.05}_{-0.04}$	$3.1^{+0.4}_{-0.4}$	$3.6^{+0.4}_{-0.4}\times10^{56}$	430^{+150}_{-170}	$0.09^{+0.03}_{-0.03}$	194
GW151012	$23.2^{+14.0}_{-5.4}$	$13.6^{+4.1}_{-4.8}$	$15.2^{+2.0}_{-1.2}$	$0.04^{+0.28}_{-0.19}$	$35.7^{+9.9}_{-3.7}$	$0.67^{+0.13}_{-0.11}$	$1.5^{+0.5}_{-0.5}$	$3.2^{+0.8}_{-1.7}\times10^{56}$	1060^{+540}_{-480}	$0.21^{+0.09}_{-0.09}$	1491
GW151226	$13.7^{+8.8}_{-3.2}$	$7.7^{+2.2}_{-2.6}$	$8.9^{+0.3}_{-0.3}$	$0.18^{+0.20}_{-0.12}$	$20.5^{+6.4}_{-1.5}$	$0.74^{+0.07}_{-0.05}$	$1.0^{+0.1}_{-0.2}$	$3.4^{+0.7}_{-1.7}\times10^{56}$	440^{+180}_{-190}	$0.09^{+0.04}_{-0.04}$	1075
GW170104	$31.0^{+7.2}_{-5.6}$	$20.1^{+4.9}_{-4.5}$	$21.5^{+2.1}_{-1.7}$	$-0.04^{+0.17}_{-0.20}$	$49.4^{+5.2}_{-3.9}$	$0.66^{+0.09}_{-0.11}$	$2.2^{+0.5}_{-0.5}$	$3.2^{+0.7}_{-1.0}\times10^{56}$	960^{+430}_{-410}	$0.19^{+0.07}_{-0.08}$	912
GW170608	$11.2^{+5.4}_{-1.9}$	$7.5^{+1.5}_{-2.1}$	$7.9^{+0.2}_{-0.2}$	$0.04^{+0.19}_{-0.06}$	$17.9^{+3.4}_{-0.7}$	$0.69^{+0.04}_{-0.04}$	$0.8^{+0.1}_{-0.1}$	$3.4^{+0.5}_{-1.3}\times10^{56}$	320^{+120}_{-110}	$0.07^{+0.02}_{-0.02}$	524
GW170729	$50.7^{+16.3}_{-10.2}$	$34.4^{+8.9}_{-10.2}$	$35.8^{+6.3}_{-4.9}$	$0.37^{+0.21}_{-0.26}$	$80.3^{+14.5}_{-10.3}$	$0.81^{+0.07}_{-0.13}$	$4.9^{+1.6}_{-1.7}$	$4.2^{+0.8}_{-1.5}\times10^{56}$	2760^{+1290}_{-1350}	$0.48^{+0.18}_{-0.21}$	1069
GW170809	$35.2^{+8.3}_{-5.9}$	$23.8^{+5.2}_{-5.1}$	$25.0^{+2.1}_{-1.6}$	$0.07^{+0.17}_{-0.16}$	$56.4^{+5.2}_{-3.7}$	$0.70^{+0.08}_{-0.09}$	$2.7^{+0.6}_{-0.6}$	$3.5^{+0.6}_{-0.9}\times10^{56}$	990^{+320}_{-380}	$0.20^{+0.05}_{-0.07}$	310
GW170814	$30.7^{+5.5}_{-2.9}$	$25.6^{+2.8}_{-4.0}$	$24.3^{+1.4}_{-1.1}$	$0.07^{+0.12}_{-0.11}$	$53.6^{+3.2}_{-2.5}$	$0.73^{+0.07}_{-0.05}$	$2.8^{+0.4}_{-0.3}$	$3.7^{+0.5}_{-0.5}\times10^{56}$	560^{+140}_{-210}	$0.12^{+0.03}_{-0.04}$	99
GW170817	$1.46^{+0.12}_{-0.10}$	$1.27^{+0.09}_{-0.09}$	$1.186^{+0.001}_{-0.001}$	$0.00^{+0.02}_{-0.01}$	≤ 2.8	≤ 0.89	≥ 0.04	$\geq 0.1\times10^{56}$	40^{+10}_{-10}	$0.01^{+0.00}_{-0.00}$	22
GW170818	$35.5^{+7.5}_{-4.7}$	$26.9^{+4.4}_{-5.2}$	$26.7^{+2.1}_{-1.7}$	$-0.09^{+0.18}_{-0.21}$	$59.8^{+4.8}_{-3.7}$	$0.67^{+0.07}_{-0.08}$	$2.7^{+0.5}_{-0.5}$	$3.4^{+0.5}_{-0.7}\times10^{56}$	1020^{+430}_{-370}	$0.20^{+0.07}_{-0.07}$	35
GW170823	$39.5^{+10.1}_{-6.6}$	$29.4^{+6.5}_{-7.1}$	$29.3^{+4.2}_{-3.1}$	$0.08^{+0.19}_{-0.22}$	$65.6^{+9.3}_{-6.5}$	$0.71^{+0.08}_{-0.09}$	$3.3^{+0.9}_{-0.8}$	$3.6^{+0.6}_{-0.9}\times10^{56}$	1860^{+840}_{-840}	$0.34^{+0.13}_{-0.14}$	1780

LIGO EGO European Gravitational Observatory LSC LIGO Scientific Collaboration VIRGO

Table of O1 and O2 triggers with source properties

See arXiv:1811.12907

Virgo data contributed to Parameter Estimation of 5 events

Event	$m_1/M_\odot$	$m_2/M_\odot$	$\mathcal{M}/M_\odot$	$\chi_{\rm eff}$	$M_{\rm f}/M_\odot$	$a_{\rm f}$	$E_{\rm rad}/(M_\odot c^2)$	$\ell_{\rm peak}/({\rm erg\ s^{-1}})$	$D_{\rm L}/{\rm Mpc}$	z	$\Delta\Omega/{\rm deg}^2$
GW150914	$35.6^{+4.8}_{-3.0}$	$30.6^{+3.0}_{-4.4}$	$28.6^{+1.6}_{-1.5}$	$-0.01^{+0.12}_{-0.13}$	$63.1^{+3.3}_{-3.0}$	$0.69^{+0.05}_{-0.04}$	$3.1^{+0.4}_{-0.4}$	$3.6^{+0.4}_{-0.4}\times10^{56}$	430^{+150}_{-170}	$0.09^{+0.03}_{-0.03}$	194
GW151012	$23.2^{+14.0}_{-5.4}$	$13.6^{+4.1}_{-4.8}$	$15.2^{+2.0}_{-1.2}$	$0.04^{+0.28}_{-0.19}$	$35.7^{+9.9}_{-3.7}$	$0.67^{+0.13}_{-0.11}$	$1.5^{+0.5}_{-0.5}$	$3.2^{+0.8}_{-1.7}\times10^{56}$	1060^{+540}_{-480}	$0.21^{+0.09}_{-0.09}$	1491
GW151226	$13.7^{+8.8}_{-3.2}$	$7.7^{+2.2}_{-2.6}$	$8.9^{+0.3}_{-0.3}$	$0.18^{+0.20}_{-0.12}$	$20.5^{+6.4}_{-1.5}$	$0.74^{+0.07}_{-0.05}$	$1.0^{+0.1}_{-0.2}$	$3.4^{+0.7}_{-1.7}\times10^{56}$	440^{+180}_{-190}	$0.09^{+0.04}_{-0.04}$	1075
GW170104	$31.0^{+7.2}_{-5.6}$	$20.1^{+4.9}_{-4.5}$	$21.5^{+2.1}_{-1.7}$	$-0.04^{+0.17}_{-0.20}$	$49.4^{+5.2}_{-3.9}$	$0.66^{+0.09}_{-0.11}$	$2.2^{+0.5}_{-0.5}$	$3.2^{+0.7}_{-1.0}\times10^{56}$	960^{+430}_{-410}	$0.19^{+0.07}_{-0.08}$	912
GW170608	$11.2^{+5.4}_{-1.9}$	$7.5^{+1.5}_{-2.1}$	$7.9^{+0.2}_{-0.2}$	$0.04^{+0.19}_{-0.06}$	$17.9^{+3.4}_{-0.7}$	$0.69^{+0.04}_{-0.04}$	$0.8^{+0.1}_{-0.1}$	$3.4^{+0.5}_{-1.3}\times10^{56}$	320^{+120}_{-110}	$0.07^{+0.02}_{-0.02}$	524
GW170729	$50.7^{+16.3}_{-10.2}$	$34.4^{+8.9}_{-10.2}$	$35.8^{+6.3}_{-4.9}$	$0.37^{+0.21}_{-0.26}$	$80.3^{+14.5}_{-10.3}$	$0.81^{+0.07}_{-0.13}$	$4.9^{+1.6}_{-1.7}$	$4.2^{+0.8}_{-1.5}\times10^{56}$	2760^{+1290}_{-1350}	$0.48^{+0.18}_{-0.21}$	1069
GW170809	$35.2^{+8.3}_{-5.9}$	$23.8^{+5.2}_{-5.1}$	$25.0^{+2.1}_{-1.6}$	$0.07^{+0.17}_{-0.16}$	$56.4^{+5.2}_{-3.7}$	$0.70^{+0.08}_{-0.09}$	$2.7^{+0.6}_{-0.6}$	$3.5^{+0.6}_{-0.9}\times10^{56}$	990^{+320}_{-380}	$0.20^{+0.05}_{-0.07}$	310
GW170814	$30.7^{+5.5}_{-2.9}$	$25.6^{+2.8}_{-4.0}$	$24.3^{+1.4}_{-1.1}$	$0.07^{+0.12}_{-0.11}$	$53.6^{+3.2}_{-2.5}$	$0.73^{+0.07}_{-0.05}$	$2.8^{+0.4}_{-0.3}$	$3.7^{+0.5}_{-0.5}\times10^{56}$	560^{+140}_{-210}	$0.12^{+0.03}_{-0.04}$	99
GW170817	$1.46^{+0.12}_{-0.10}$	$1.27^{+0.09}_{-0.09}$	$1.186^{+0.001}_{-0.001}$	$0.00^{+0.02}_{-0.01}$	≤ 2.8	≤ 0.89	≥ 0.04	$\geq 0.1\times10^{56}$	40^{+10}_{-10}	$0.01^{+0.00}_{-0.00}$	22
GW170818	$35.5^{+7.5}_{-4.7}$	$26.9^{+4.4}_{-5.2}$	$26.7^{+2.1}_{-1.7}$	$-0.09^{+0.18}_{-0.21}$	$59.8^{+4.8}_{-3.7}$	$0.67^{+0.07}_{-0.08}$	$2.7^{+0.5}_{-0.5}$	$3.4^{+0.5}_{-0.7}\times10^{56}$	1020^{+430}_{-370}	$0.20^{+0.07}_{-0.07}$	35
GW170823	$39.5^{+10.1}_{-6.6}$	$29.4^{+6.5}_{-7.1}$	$29.3^{+4.2}_{-3.1}$	$0.08^{+0.19}_{-0.22}$	$65.6^{+9.3}_{-6.5}$	$0.71^{+0.08}_{-0.09}$	$3.3^{+0.9}_{-0.8}$	$3.6^{+0.6}_{-0.9}\times10^{56}$	1860^{+840}_{-840}	$0.34^{+0.13}_{-0.14}$	1780

LIGO EGO European Gravitational Observatory LSC LIGO Scientific Collaboration VIRGO

Some remarks

Properties of black holes and neutron stars from transients

Extract information on masses, spins, energy radiated, position, distance, inclination, polarization. Population distribution may shed light on formation mechanisms

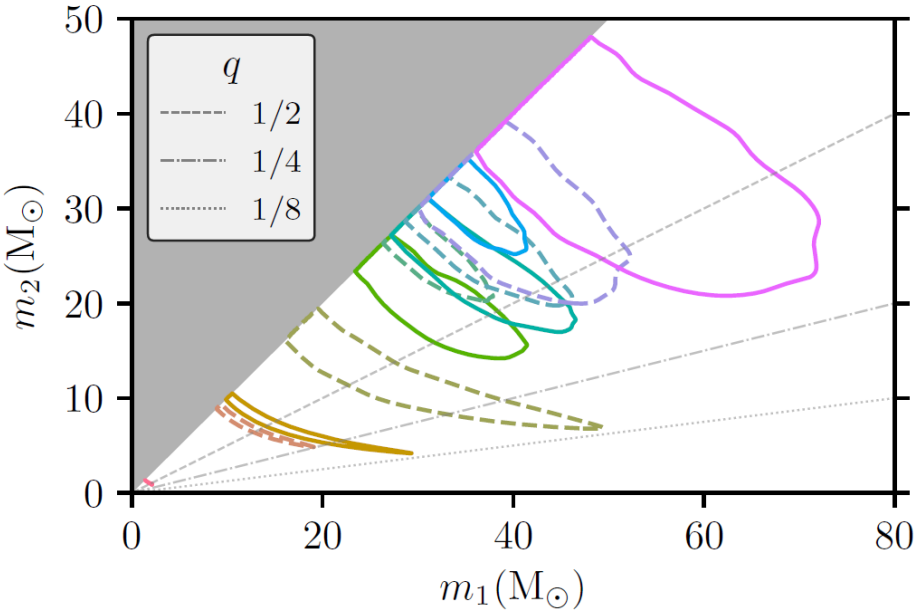

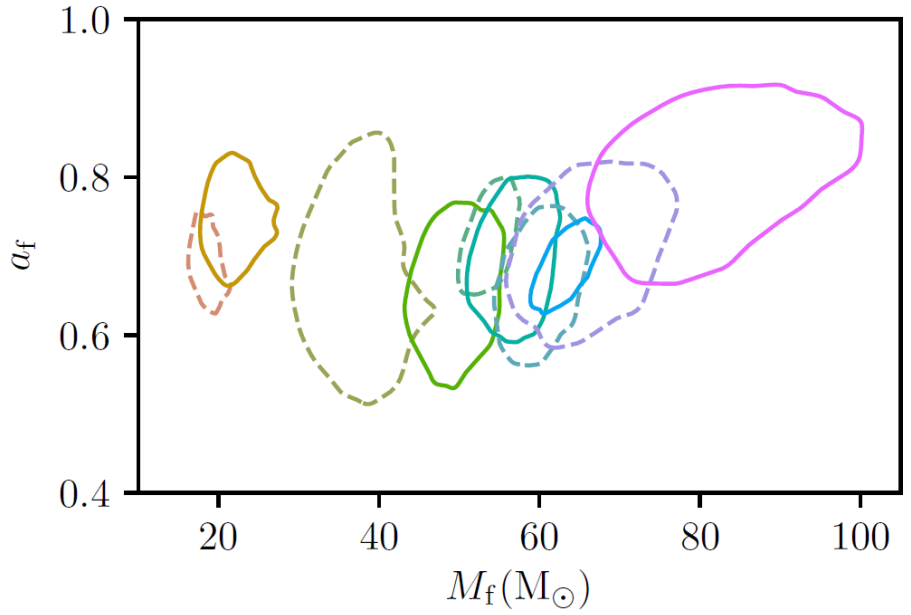

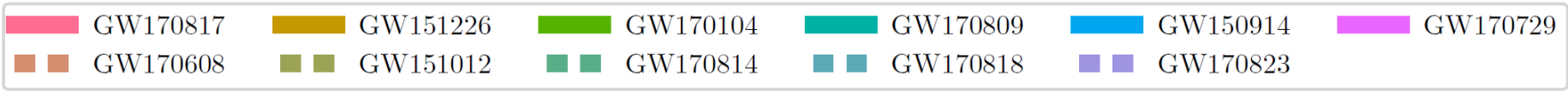

"GWTC-1: A Gravitational-Wave Transient Catalog of Compact Binary Mergers Observed by LIGO and Virgo during the First and Second Observing Runs", The LIGO Virgo Collaboration, arXiv:1811.12907

LIGO-Virgo analyses for sources of gravitational waves

Sources can be transient or of continuous nature, and can be modeled or unmodeled

Coalescence of Compact Sources

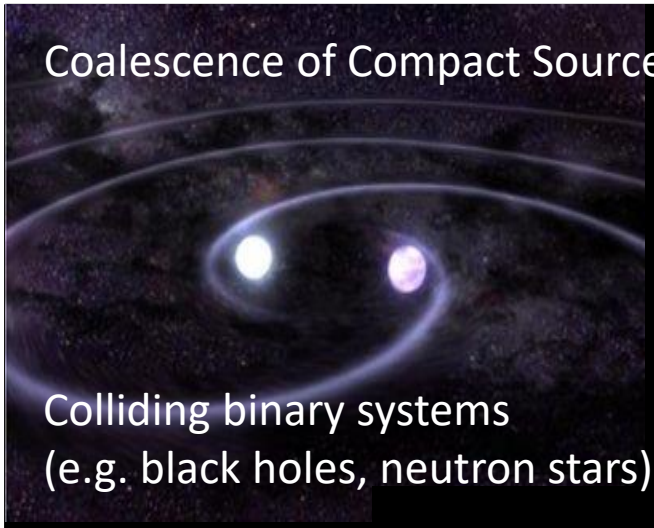

Colliding binary systems
(e.g. black holes, neutron stars)

Continuous Waves

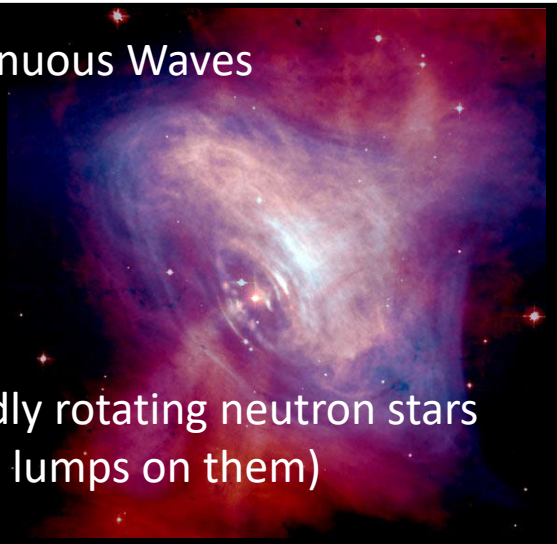

Rapidly rotating neutron stars
(with lumps on them)

Burst

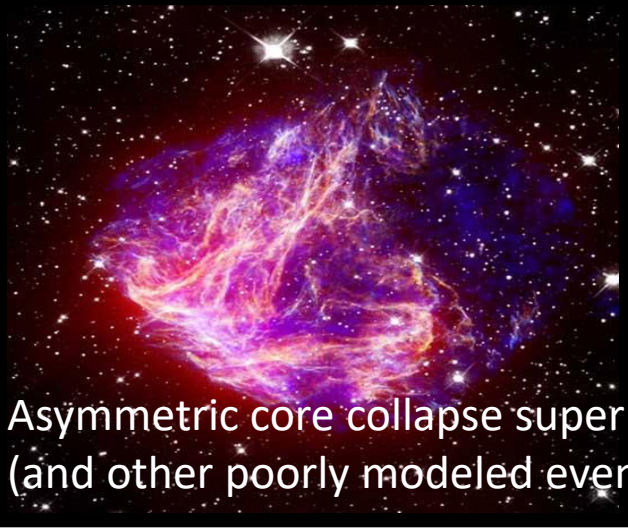

Asymmetric core collapse supernovae
(and other poorly modeled events)

Stochastic

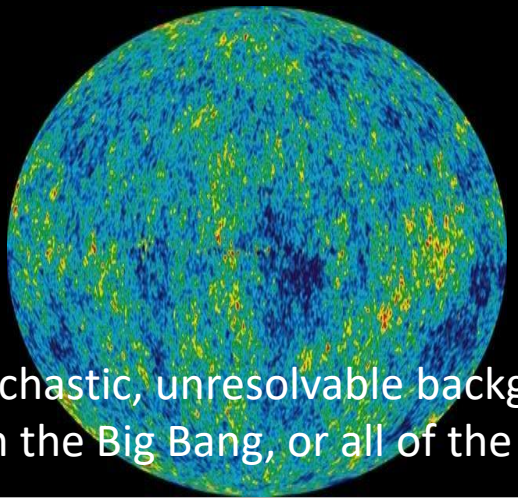

A stochastic, unresolvable background
(from the Big Bang, or all of the above)

Source parameters for the first event: GW150914

Estimated masses (90% probability intervals) for the two black holes in the binary (m_1^{source} is the mass of the heavier black hole). Different curves show different models. Mass and spin of the final black hole

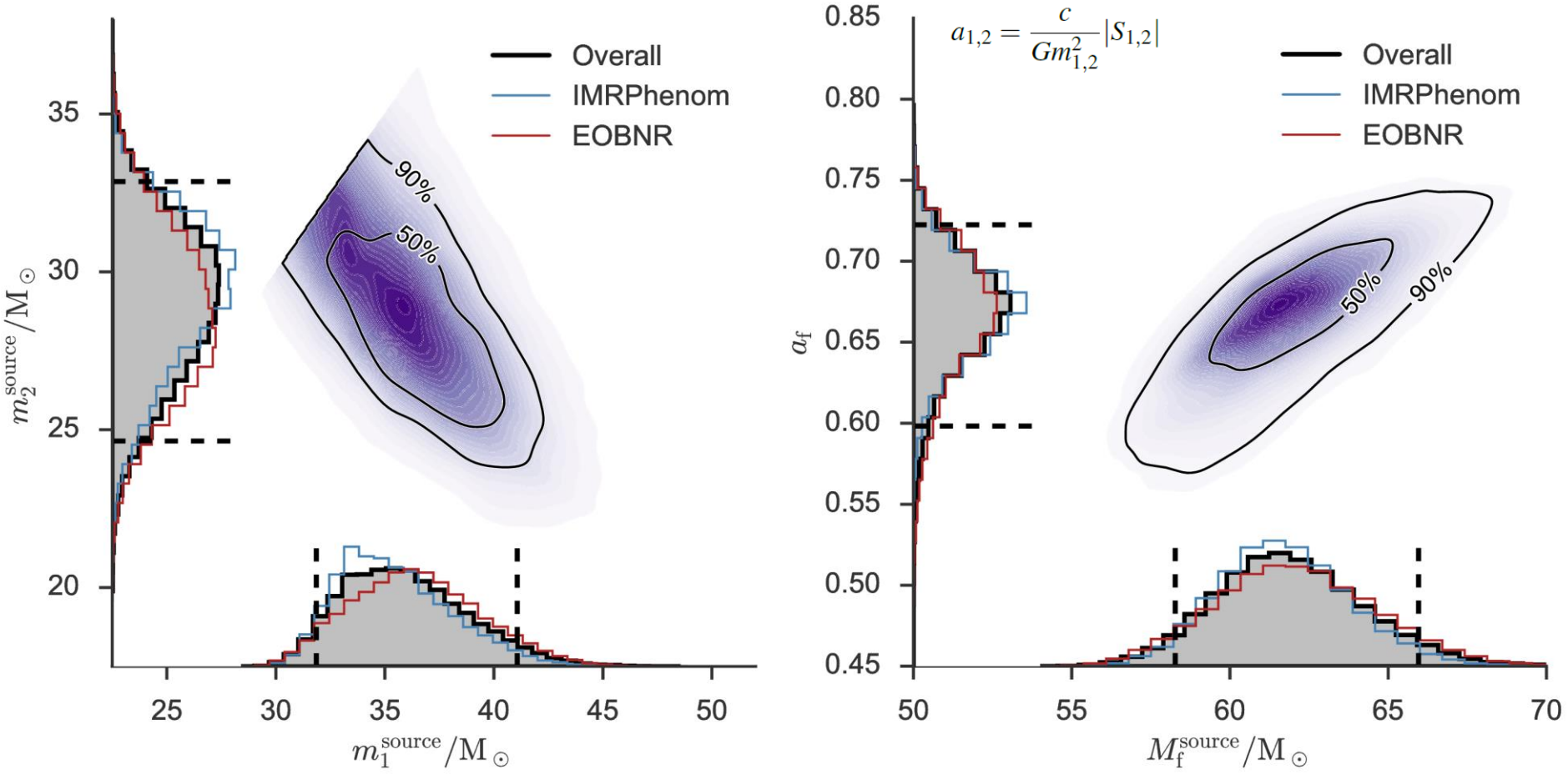

Energy radiated: 3.0 ± 0.5 solar masses. Peak power at merger: 200 solar masses per second

See "*Properties of the Binary Black Hole Merger GW150914*" http://arxiv.org/abs/1602.03840

Luminosity distance to the source

Estimated luminosity distance and binary inclination angle. An inclination of $\theta_{JN} = 90^{\circ}$ means we are looking at the binary (approximately) edge-on. Again 90% credible level contours

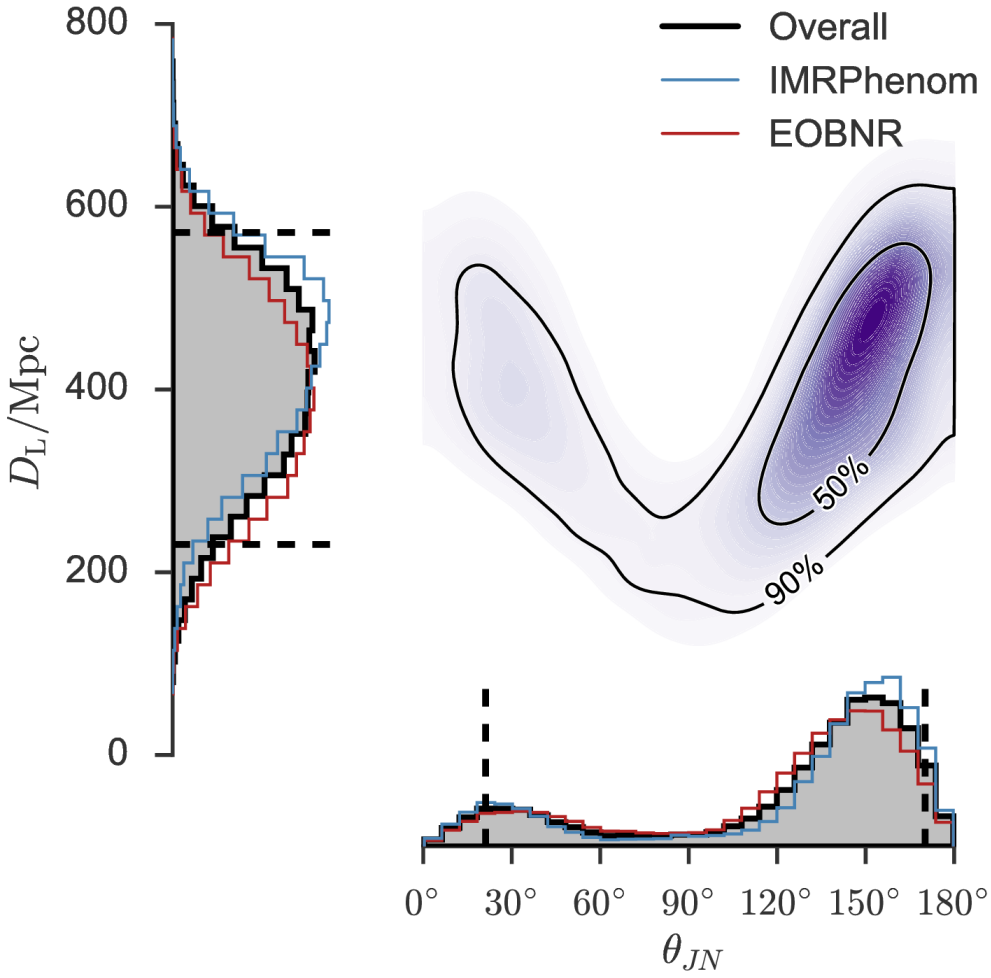

Polarization can be used to break the degeneracy between distance and inclination

$$h_+ = \frac{2\nu M}{d}[\pi M f(t)]^{2/3}\left(1+\cos^2\iota\right)\cos[2\varphi(t)]$$

$$h_\times = \frac{4\nu M}{d}[\pi M f(t)]^{2/3}\cos\iota\,\sin[2\varphi(t)]$$

To measure the polarization components, we need a third detector, i.e. Virgo, oriented at about 45 degrees with respect to LIGO

Fundamental physics: polarization of gravitational waves

Polarization is a fundamental property of spacetime. It determined how spacetime can be deformed. General metric theories allow six polarizations. General Relativity allows two (tensor) polarizations

GR only allows (T) polarizations

General metric theories also know
vector (V) and scalar (S) polarizations

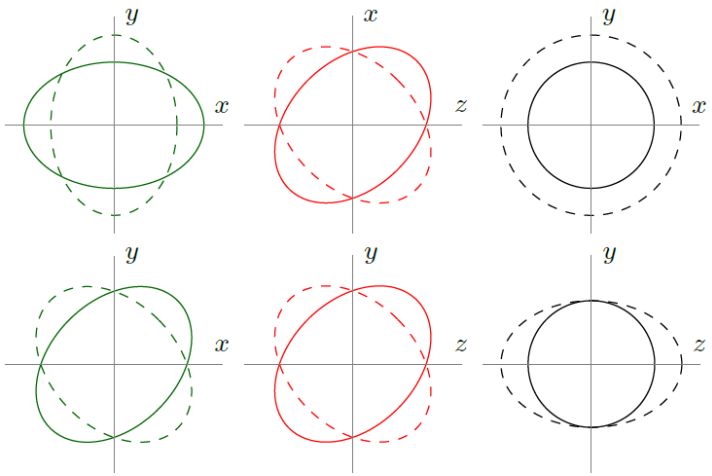

Theory	+	x	x	y	b	l
General Relativity						
GR in noncompactified 4/6D Minkowski						
Einstein-Æther						
5D Kaluza-Klein						
Randall-Sundrum braneworld						
Dvali-Gabadadze-Porrati braneworld						
Brans-Dicke						
f(R) gravity						
Bimetric theory						
Four-Vector Gravity						

Nishizawa et al., Phys. Rev. D 79, 082002 (2009) [except G4v & Einstein-Æther].

allowed / depends / forbidden

GW170814: first test of polarizations of GW

According to Einstein's General Relativity there exist only two polarizations. General metric theories of gravity allow six polarizations. GW170814 confirms Einstein's prediction

Angular dependence (antenna-pattern) differs for T, V, S

LIGO and Virgo have different antenna-patterns
This allows for fundamental test of the polarizations of spacetime

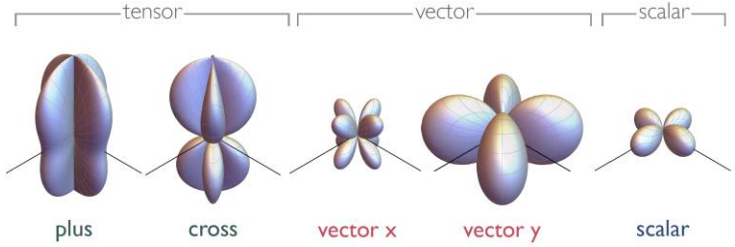

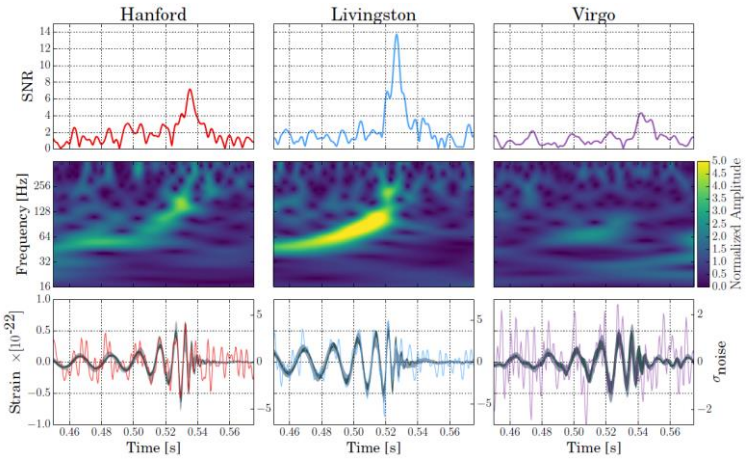

Our analysis favors tensor polarizations in support of General Relativity

Our data favor tensor structure over vector by about a (Bayes) factor 200

And tensor over scalar by about a factor 1000

This is a first test, and for BBH we do not know the source position very well

Combinations of component spins for GW150914

GW150914 suggests that the individual spins were either small, or they were pointed opposite from one another, cancelling each other's effect. Spin maybe the key to understanding formation channels

Precession is an important clue into how the black holes formed. If there is not any precession it is more likely that the black holes formed together. If there is a lot of precession it is more likely that the black holes formed separately and before coming together

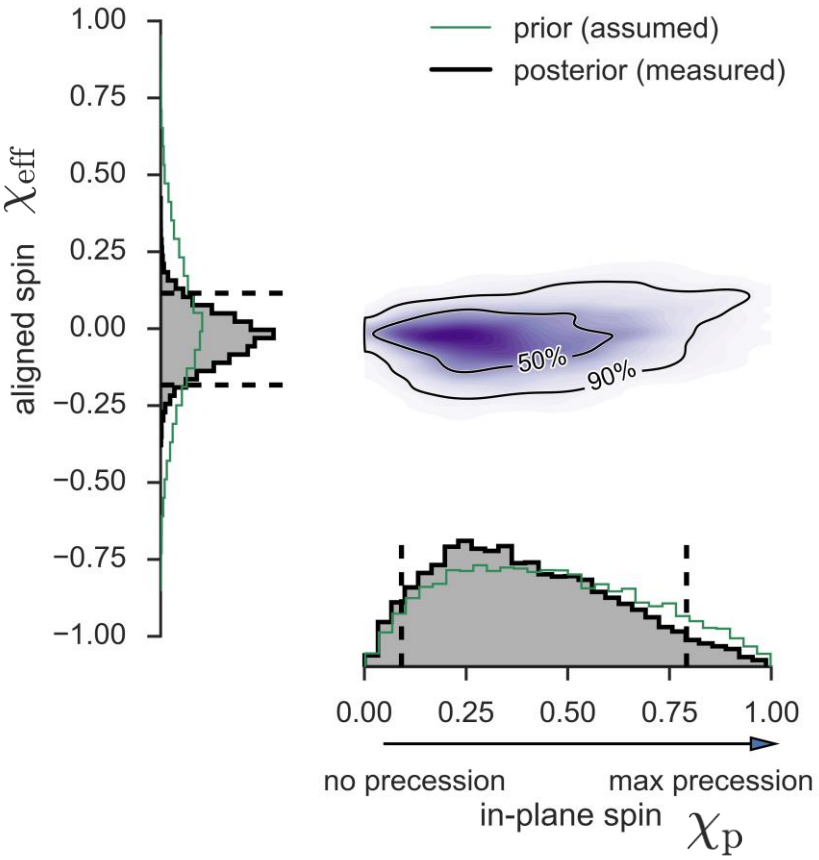

Effective spin parameter

$$\chi_{\rm eff} = \frac{c}{GM}\left(\frac{\boldsymbol{S}_1}{m_1} + \frac{\boldsymbol{S}_2}{m_2}\right)\cdot\frac{\boldsymbol{L}}{|\mathbf{L}|}$$

Precession in BBH

$$\dot{\boldsymbol{L}} = \frac{G}{c^2 r^3}(B_1\boldsymbol{S}_{1\perp} + B_2\boldsymbol{S}_{2\perp})\times\boldsymbol{L}$$

$$\dot{\boldsymbol{S}}_i = \frac{G}{c^2 r^3}B_i\boldsymbol{L}\times\boldsymbol{S}_i,$$

Effective precession spin parameter

$$\chi_p = \frac{c}{B_1 G m_1^2}\max(B_1 S_{1\perp}, B_2 S_{2\perp}) > 0$$

$\chi_p = 0$ aligned-spin (non-precessing) system

$$B_1 = 2 + 3q/2 \text{ and } B_2 = 2 + 3/(2q), \text{ and } i = \{1, 2\}$$

See "*Properties of the Binary Black Hole Merger GW150914*" http://arxiv.org/abs/1602.03840

Effect of orientation of binary's orbital plane

Polarization of gravitational waves depends on the orientation of the orbital plan of the binary system. Face-on we observe a mixture, while edge-on we observe pure h+

Spinning, but non-precessing binary

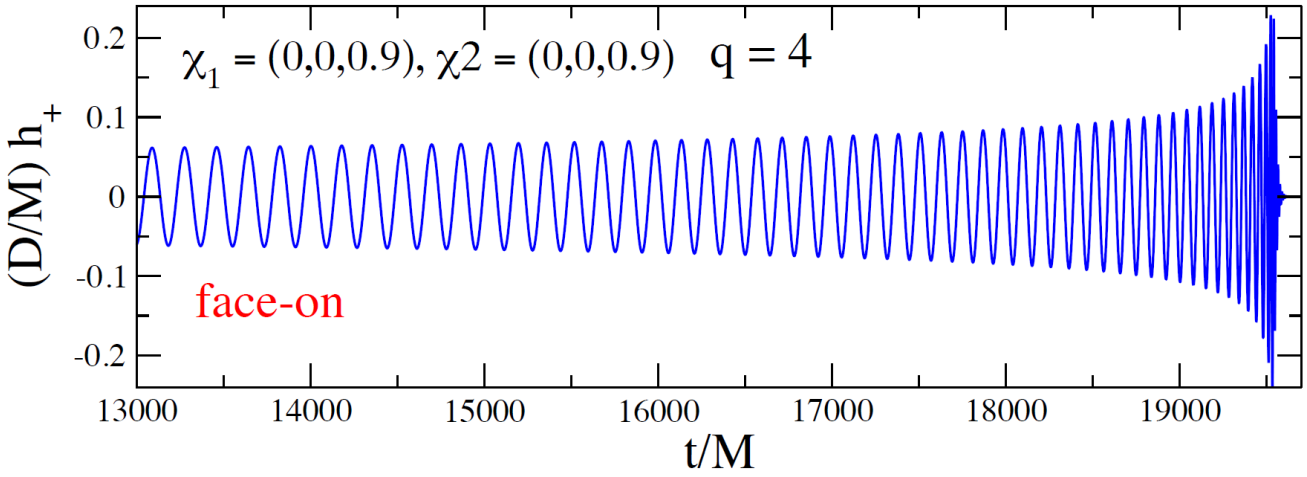

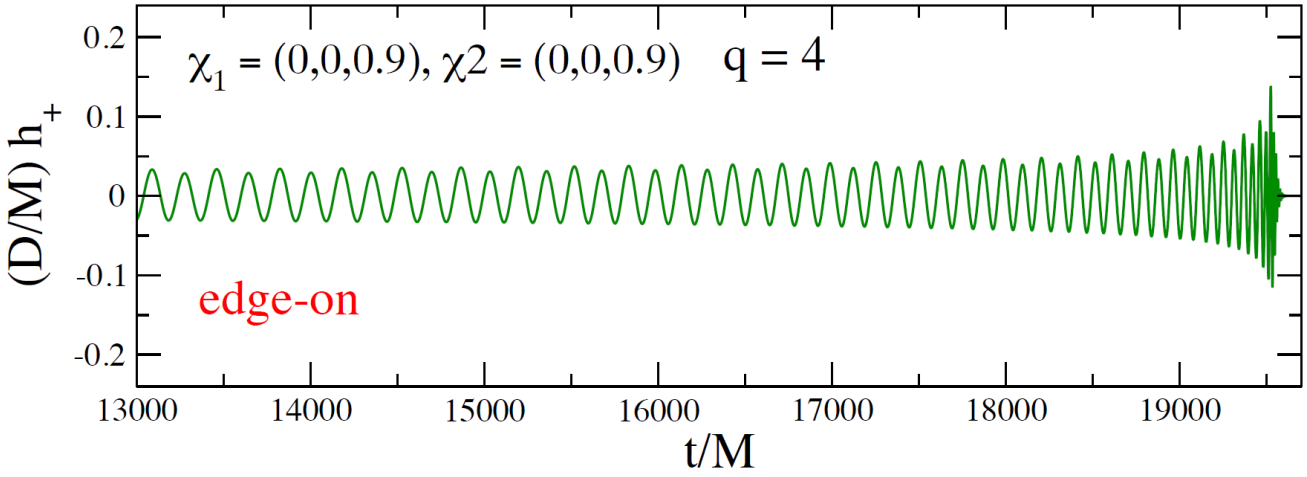

Effect of orientation of binary's orbital plane

Spin precession leads to amplitude and frequency modulation

Having good low frequency sensitivity will enable observing precession effects

Spin-precessing binary

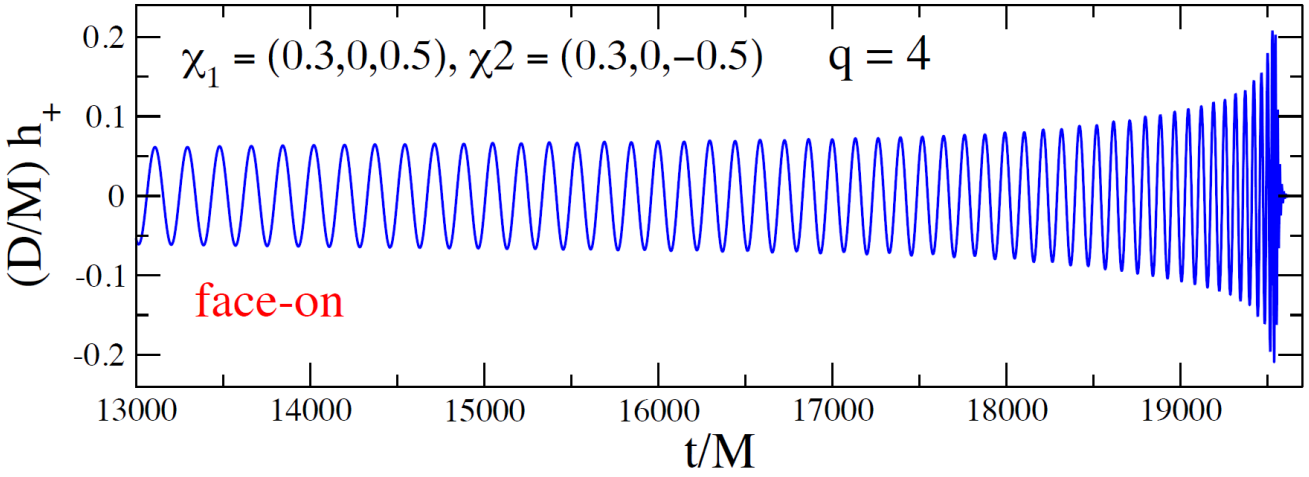

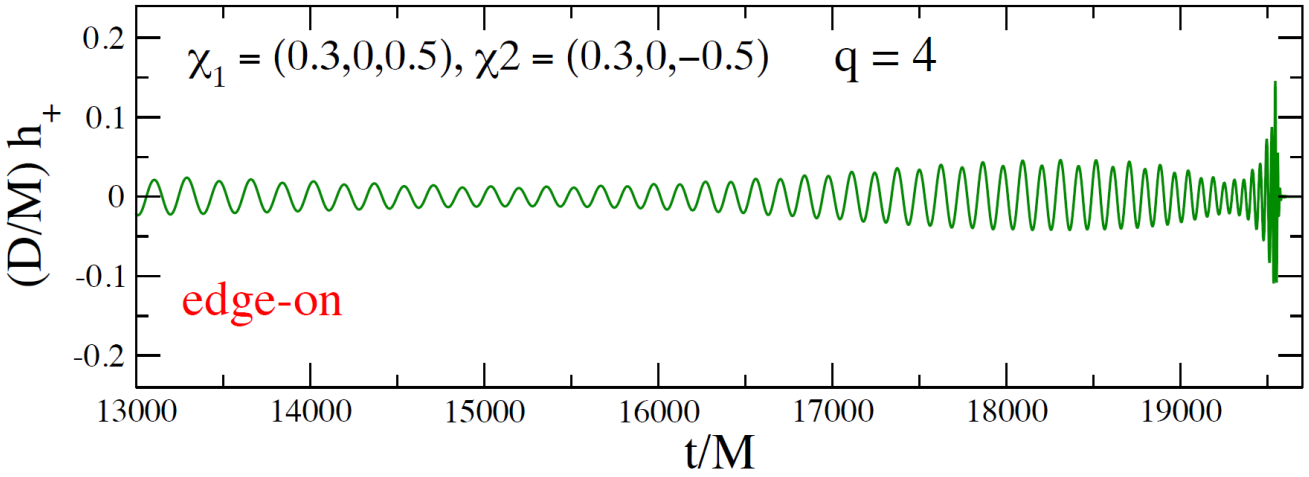

In-band time T is related to the low-frequency cut off frequency $T \approx \left(\frac{1}{f_0}\right)^{8/3}$

Intermediate mass black hole binaries

Having good low frequency sensitivity will enable assessing the population of IMBHB.
LVC has put an limit on the probability of the IMBHB distribution

Search for intermediate mass black hole binaries in the first and second observing runs of the Advanced LIGO and Virgo network

(Dated: July 3, 2019)

Gravitational wave astronomy has been firmly established with the detection of gravitational waves from the merger of ten stellar mass binary black holes and a neutron star binary. This paper reports on the all-sky search for gravitational waves from intermediate mass black hole binaries in the first and second observing runs of the Advanced LIGO and Virgo network. The search uses three independent algorithms: two based on matched filtering of the data with waveform templates of gravitational wave signals from compact binaries, and a third, model-independent algorithm that employs no signal model for the incoming signal. No intermediate mass black hole binary event was detected in this search. Consequently, we place upper limits on the merger rate density for a family of intermediate mass black hole binaries. In particular, we choose sources with total masses $M = m_1 + m_2 \in [120, 800]$ $M_\odot$ and mass ratios $q = m_2/m_1 \in [0.1, 1.0]$. For the first time, this calculation is done using numerical relativity waveforms (which include higher modes) as models of the real emitted signal. We place a most stringent upper limit of 0.20 $\mathrm{Gpc}^{-3}\mathrm{yr}^{-1}$ (in co-moving units at the 90% confidence level) for equal-mass binaries with individual masses $m_{1,2} = 100$ $M_\odot$ and dimensionless spins $\chi_{1,2} = 0.8$ aligned with the orbital angular momentum of the binary. This improves by a factor of ~ 5 that reported after Advanced LIGO's first observing run.

PACS numbers: 04.80.Nn, 07.05.Kf, 95.55.Ym

Precision tests of GR with BBH mergers

Bayesian analysis increases accuracy on parameters by combining information from multiple events

Inspiral and PN expansion

Inspiral PN and logarithmic terms: Sensitive to GW back-reaction, spin-orbit, spin-spin couplings, …

Orbital phase (post Newtonian expansion): $h^{\alpha\beta}(f) = h^{\alpha\beta} e^{i\Phi(f)}$

$$\Phi(v) = \left(\frac{v}{c}\right)^{-5} \sum_{n=0}^{\infty} \left[\varphi_n + \varphi_n^{(l)} \ln\left(\frac{v}{c}\right)\right] \left(\frac{v}{c}\right)^n$$

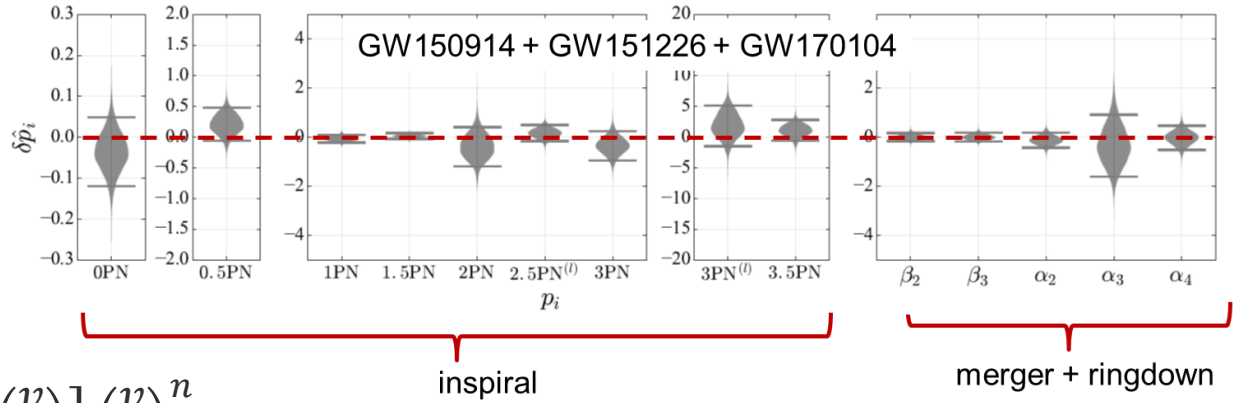

Merger terms: numerical GR

Ringdown terms: quasi-normal modes; do we see Kerr black holes?

Towards high precision tests of gravity

Combining information from multiple events and having high-SNR events will allow unprecedented tests of GR and other theories of gravity

Our collaborations set ambitious goals for the future

We need to improve:

- sensitivity of our instruments over the entire frequency range
- optimize our computing and analysis
- improve our source modeling (NR)

Is a black hole created in the final state?

From the inspiral we can predict that the ringdown frequency of about 250 Hz and 4 ms decay time. This is what we measure (http://arxiv.org/abs/1602.03841). We will pursue this further and perform test of no-hair theorem. This demands good sensitivity at high frequency

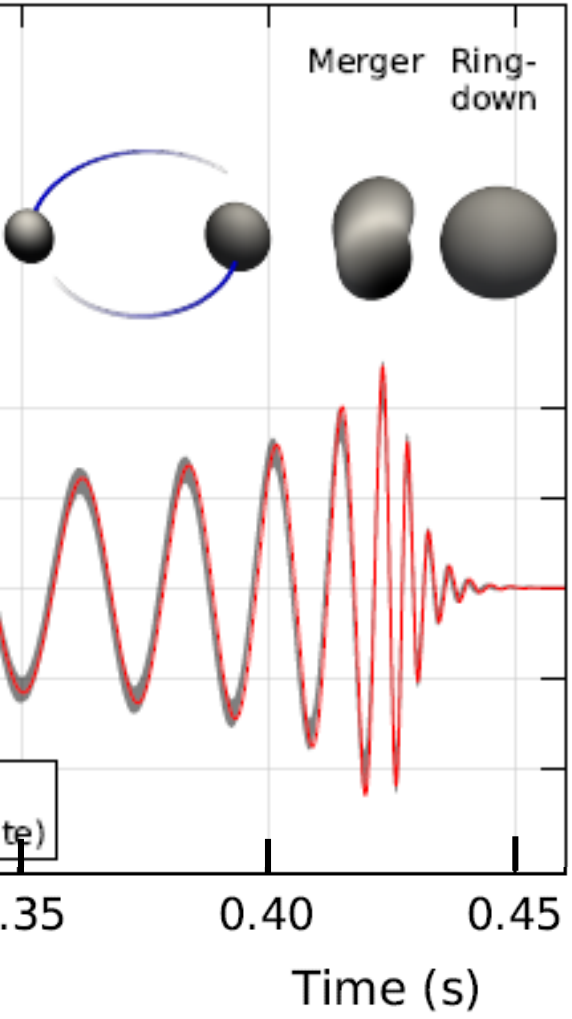

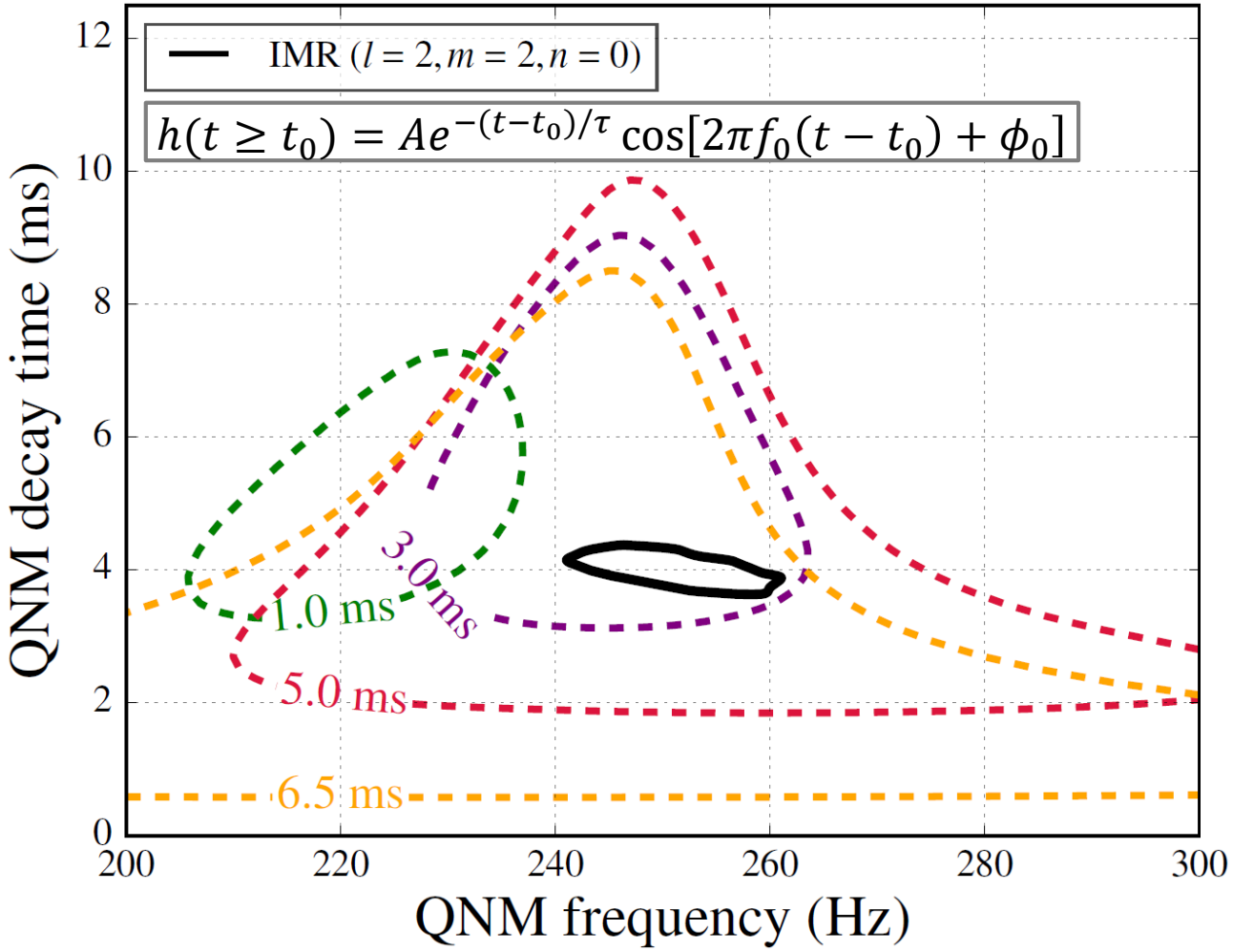

Exotic compact objects

Gravitational waves from coalescence of two compact objects is the Rosetta Stone of the strong-field regime. It may hold the key and provide an in-depth probe of the nature of spacetime

Quantum modifications of GR black holes

- Motivated by Hawking's information paradox
- Firewalls, fuzzballs, EP = EPR, …

Fermionic dark matter

- Dark matter stars

Boson stars

- Macroscopic objects made up of scalar fields

Gravastars

- Objects with de Sitter core where spacetime is self-repulsive
- Held together by a shell of matter
- Relatively low entropy object

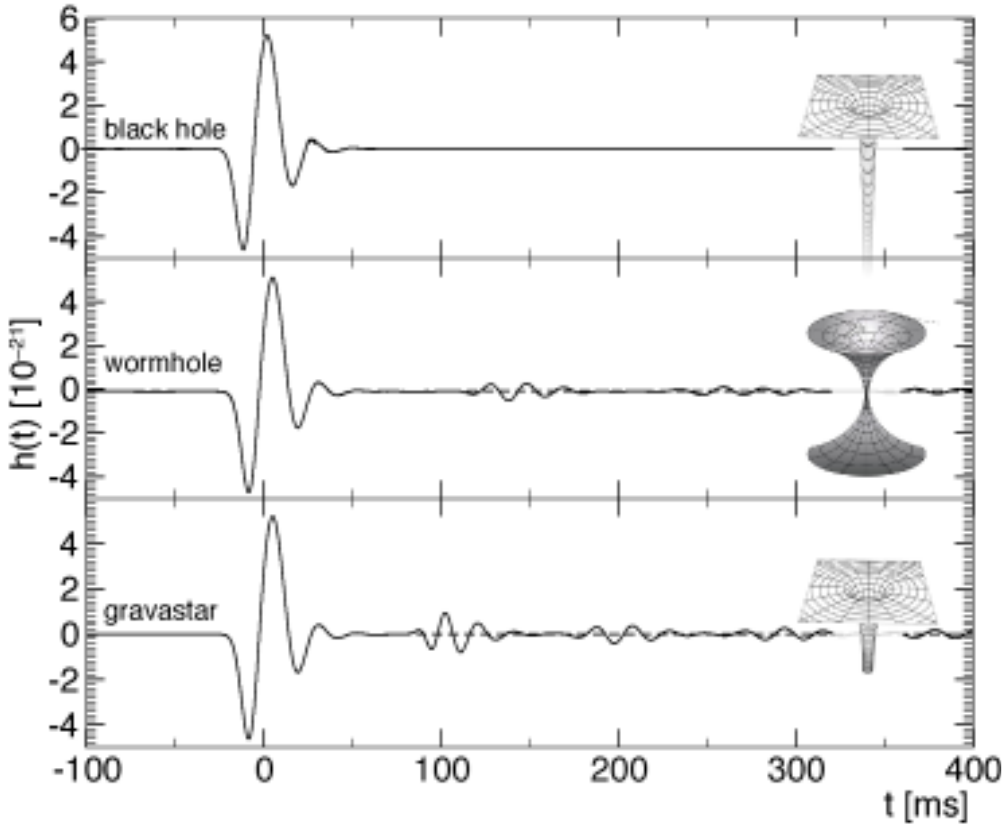

GW observables

- Inspiral signal: modifications due to tidal deformation effects
- Ringdown process: use QNM to check no-hair theorem
- Echoes: even for Planck-scale corrections $\Delta t \approx -nM \log \frac{l}{M}$
- Studies require good sensitivity at high frequency

Limit on the mass of the graviton

Bounds on the Compton wavelength $\lambda_g = {}^{h}/_{m_g c}$ of the graviton compared to Solar System or double pulsar tests. Some cosmological tests are stronger (but make assumptions about dark matter)

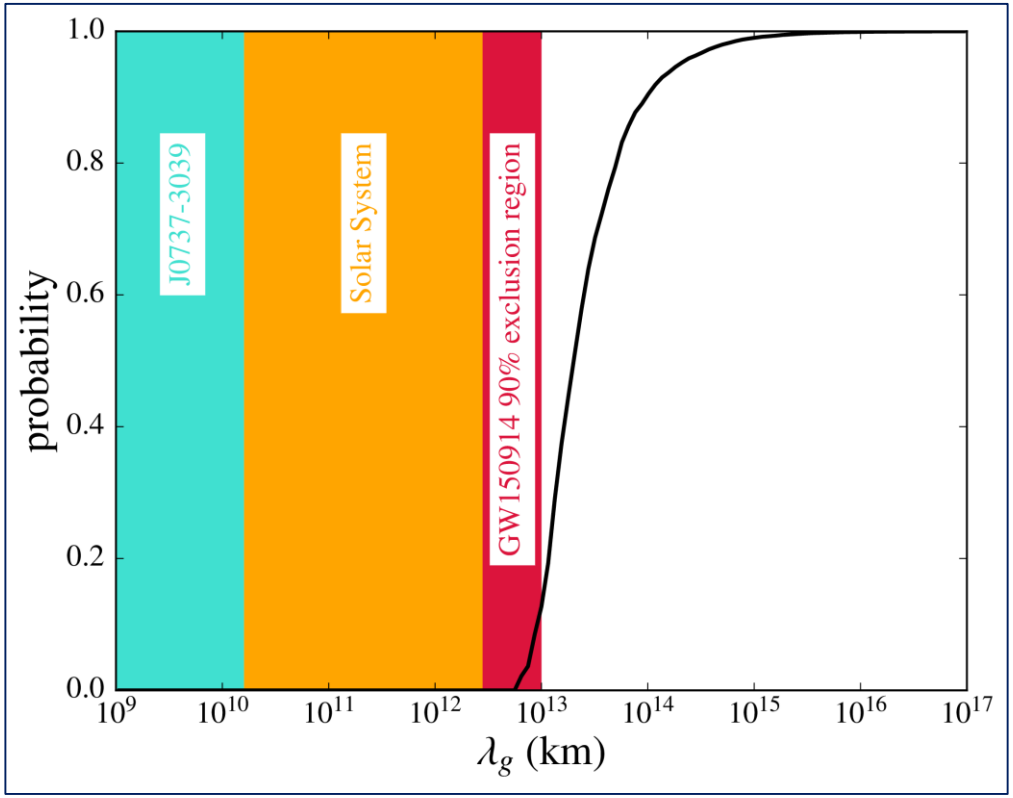

See "*Tests of general relativity with GW150914*" http://arxiv.org/abs/1602.03841

$$\delta\Phi(f) = -\frac{\pi D c}{\lambda_g^2(1+z)} f^{-1}$$

Will, Phys. Rev. D **57**, 2061 (1998)

Massive-graviton theory dispersion relation $E^2 = p^2c^2 + m_g^2c^4$

We have $\lambda_g = h/(m_g c)$

Thus frequency dependent speed

$$\frac{v_g^2}{c^2} \equiv \frac{c^2p^2}{E^2} \cong 1 - h^2c^2/(\lambda_g^2 E^2)$$

$\lambda_g > 10^{13}$ km

$m_g \leq 10^{-22}\mathrm{eV/c^2}$

Bounds on violation of Lorentz invariance

First bounds derived from gravitational-wave observations, and the first tests of superluminal propagation in the gravitational sector

Generic dispersion relation $$E^2 = p^2c^2 + Ap^\alpha c^\alpha, \alpha \geq 0 \Rightarrow \frac{v_g}{c} \cong 1 + (\alpha - 1)AE^{\alpha-2}/2$$

Gravitational wave phase term $$\delta\Psi = \begin{cases} \frac{\pi}{\alpha-1}\frac{AD_\alpha}{(hc)^{2-\alpha}}\left[\frac{(1+z)f}{c}\right]^{\alpha-1} & \alpha \neq 1 \\ \frac{\pi AD_\alpha}{hc}\ln\left(\frac{\pi G\mathcal{M}^{det}f}{c^3}\right) & \alpha = 1 \end{cases} \qquad A \cong \pm\frac{MD_\alpha}{\lambda_A^2}$$

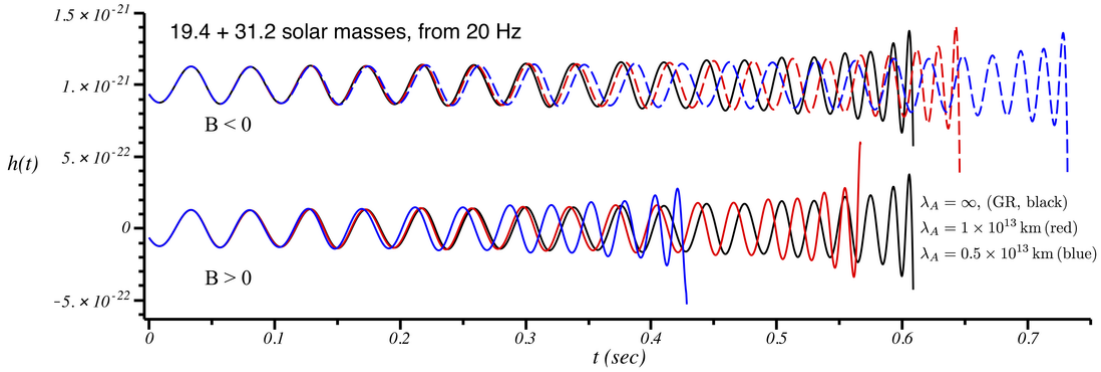

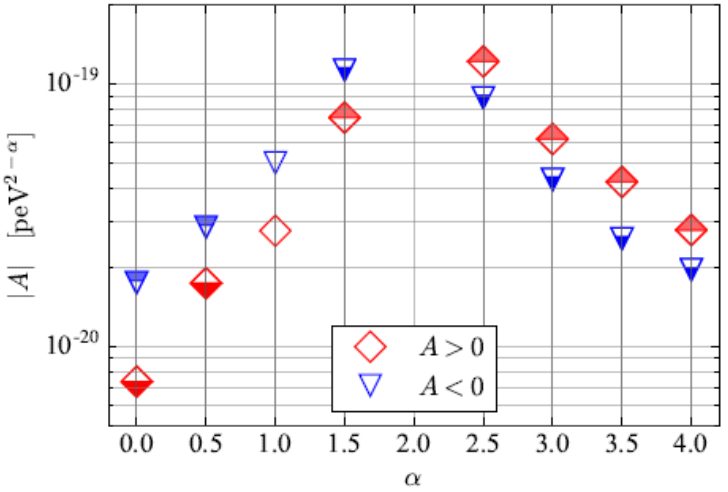

Several modified theories of gravity predict specific values of α:
- massive-graviton theories (α = 0, A > 0), multifractal spacetime (α = 2.5),
- doubly special relativity (α = 3), and Horava-Lifshitz and extradimensional theories (α = 4)

Virgo allowed source location via triangulation

GW170817 first arrived at Virgo, after 22 ms it arrived at LLO, and another 3 ms later LLH detected it

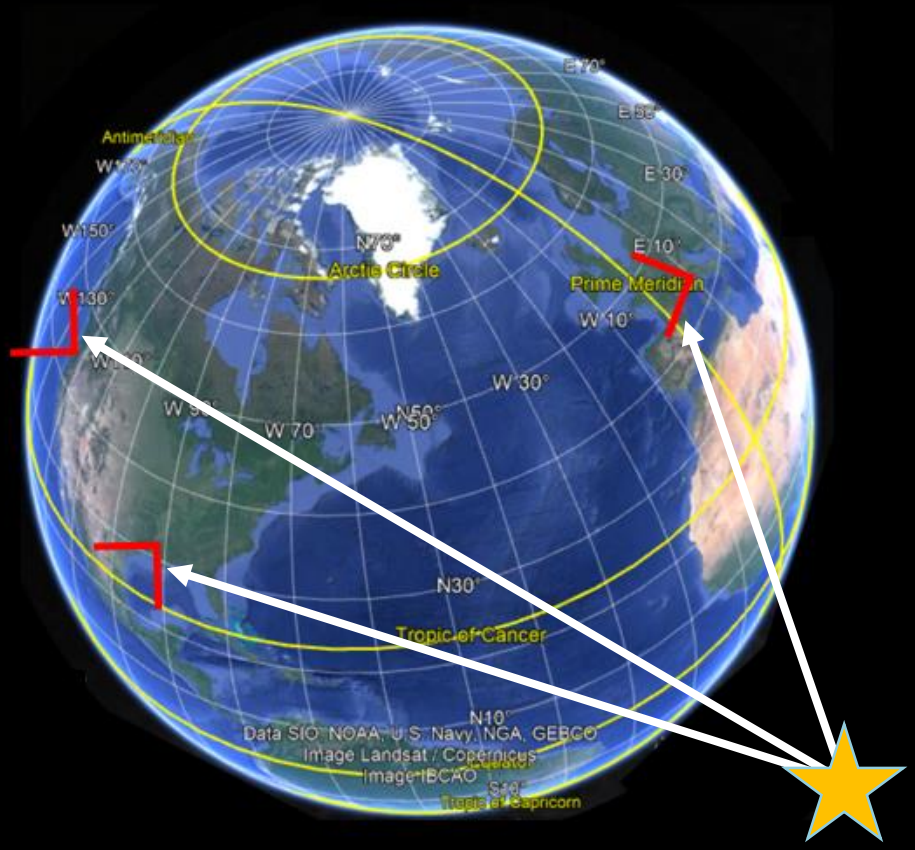

Distributed skymaps

See https://dcc.ligo.org/LIGO-G1801864

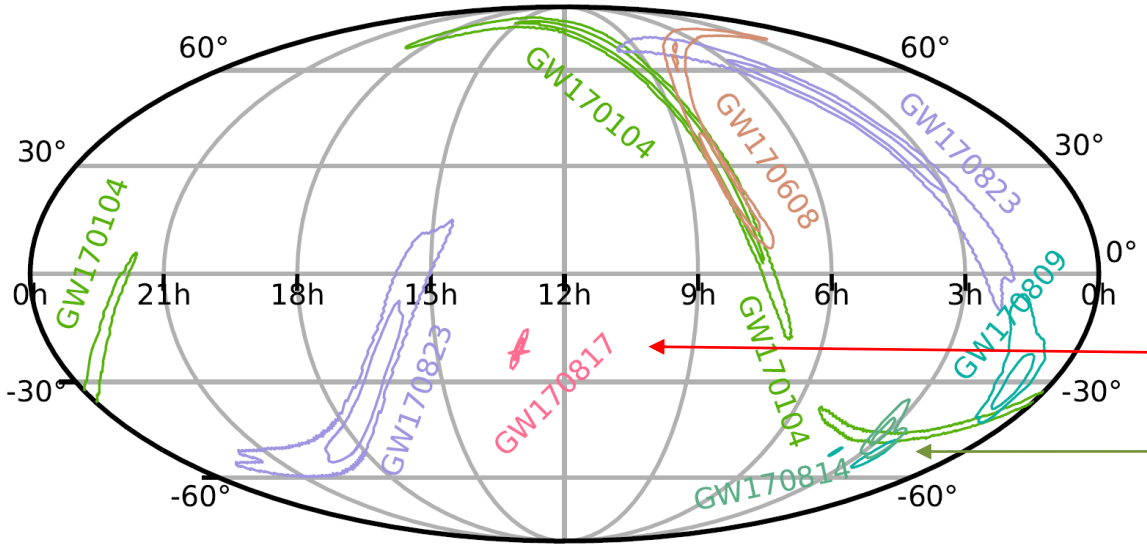

GW170817

GW170814

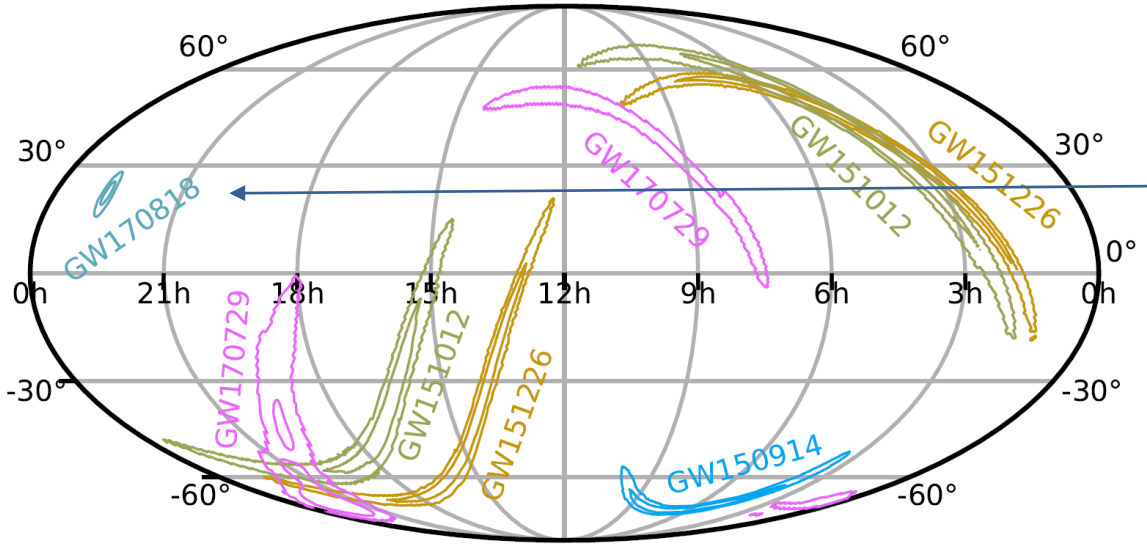

GW170818

LSC LIGO Scientific Collaboration

VIRGO

Multi-messenger astronomy

Looking into the heart of a dim nearby sGRB

Gravitational waves identified the progenitor of the sGRB and provided both space localization and distance of the source. This triggered the EM follow-up by astronomers for the kilonova

Closest by and weakest sGRB, highest SNR GW event

LIGO/Virgo network allowed source localization of 16 (degr)^2 at 90% CL
and distance measurement of about 40 Mpc

Source localization requires better high frequency sensitivity

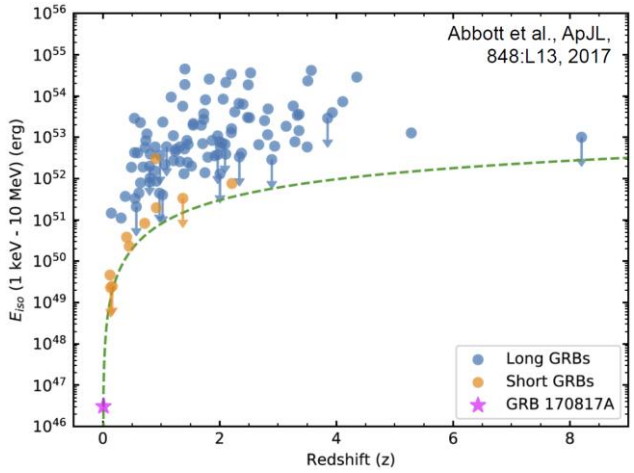

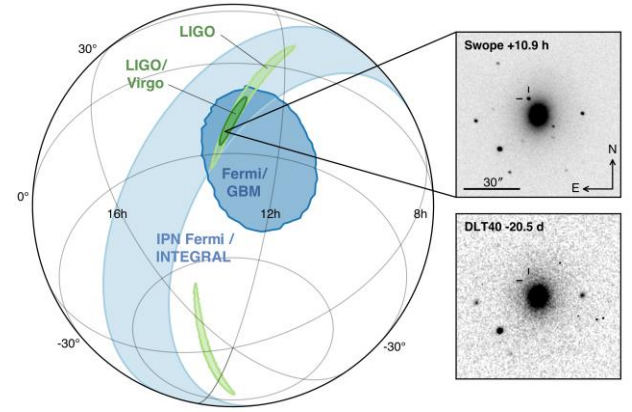

Multi-messenger astronomy and future early warning

ePESSTO and VLT xshooter spectra with TARDIS radiative transfer models
See Smartt S.J. *et al*., Nature, 551, 75-79, 2017 for more details

The kilonova essentially has a black-body spectrum (6000 K; blue curve in panel C)

Data shows evidence for absorption lines (see model with tellurium and cesium with atomic numbers 52 and 55)

Formation of Cs and Te is difficult to explain in supernova explosions

The lines are Doppler broadened due to the high speed of the ejected material (about 60,000 km/s)

Early warning will profit from better low-frequency sensitivity

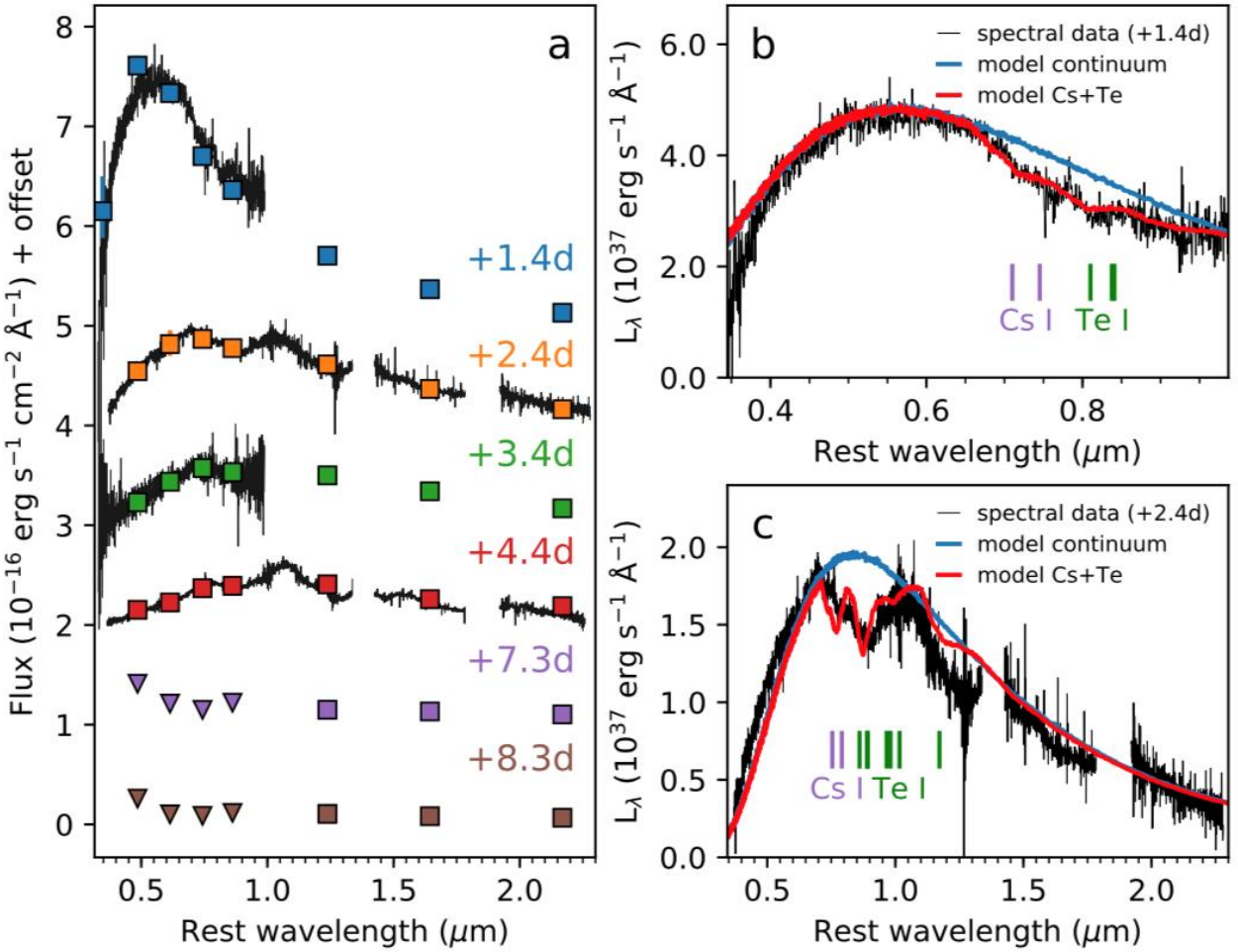

GW170817 properties: tidal deformability, EOS, radii

Tidal deformability gives support for “soft” EOS, leading to more compact NS. Various models can now be excluded. We can place the additional constraint that the EOS must support a NS $1.97\,\mathrm{M}_\odot$

Leading tidal contribution to GW phase appears at 5 PN: $\tilde{\Lambda} = \frac{16}{13}\frac{(m_1+12m_2)m_1^4\Lambda_1 + (m_2+12m_1)m_2^4\Lambda_2}{(m_1+m_2)^5}$

Tidal effects due to neutron star structure profit from high frequency sensitivity

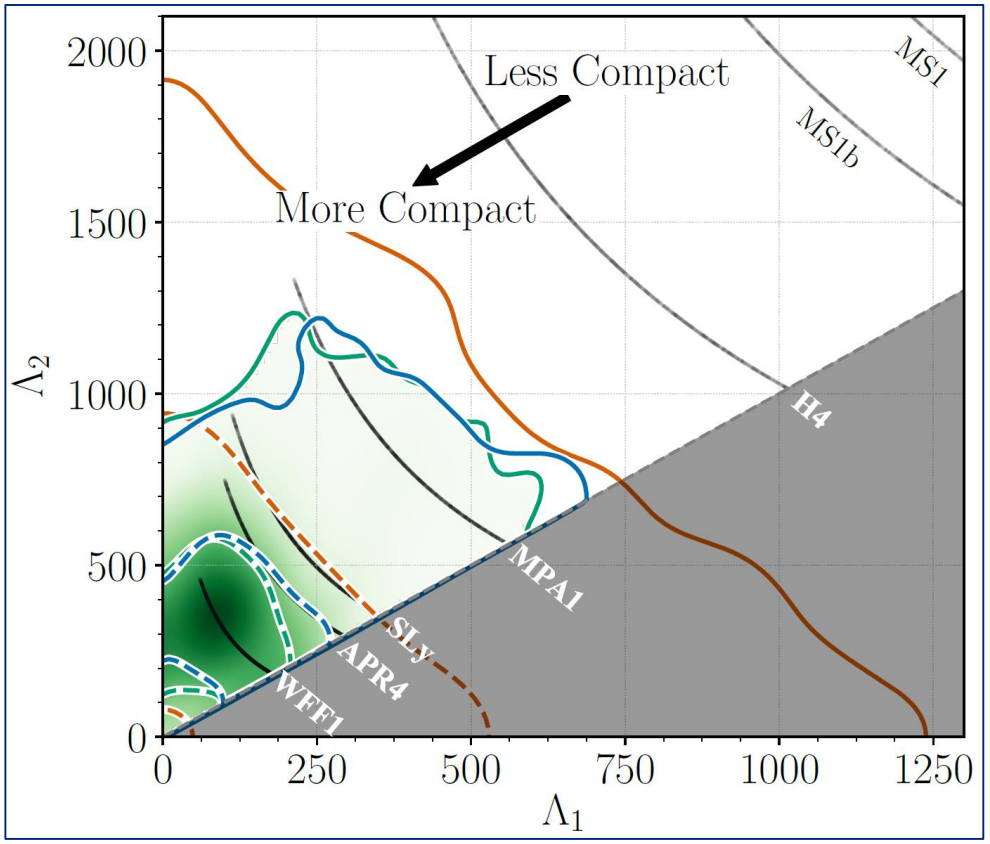

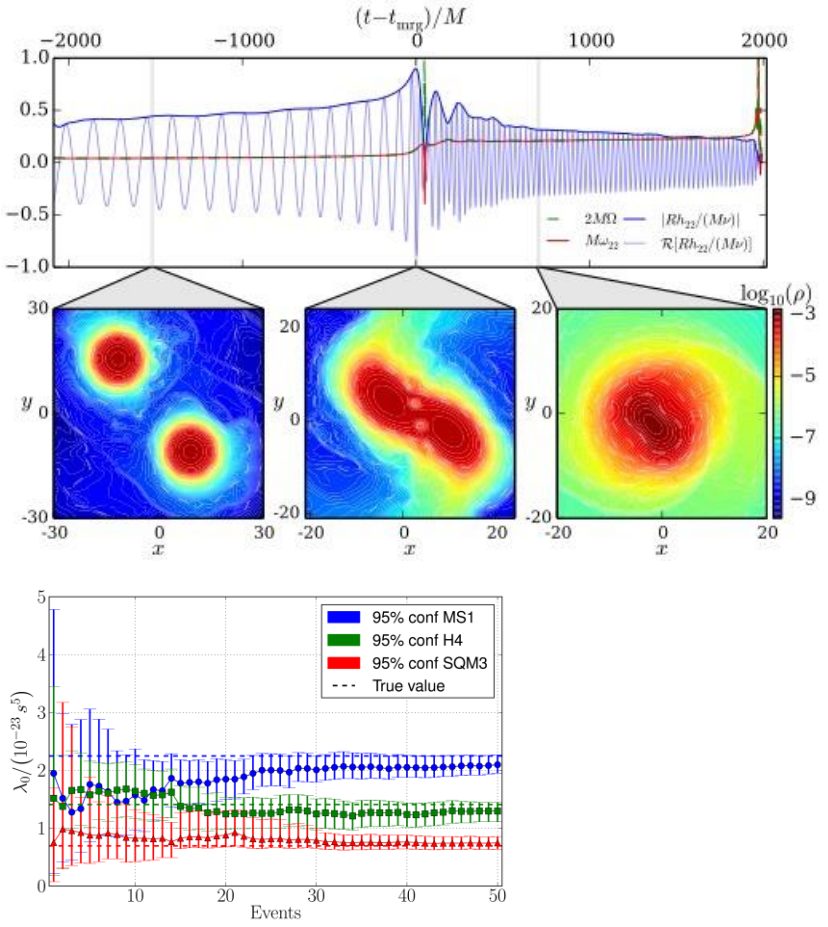

A new cosmic distance marker

Binary neutron stars allow a new way of mapping out the large-scale structure and evolution of spacetime by comparing distance and redshift

Current measurements depend on cosmic distance ladder

- Intrinsic brightness of *e.g.* supernovae determined by comparison with different, closer-by objects
- Possibility of systematic errors at every “rung” of the ladder

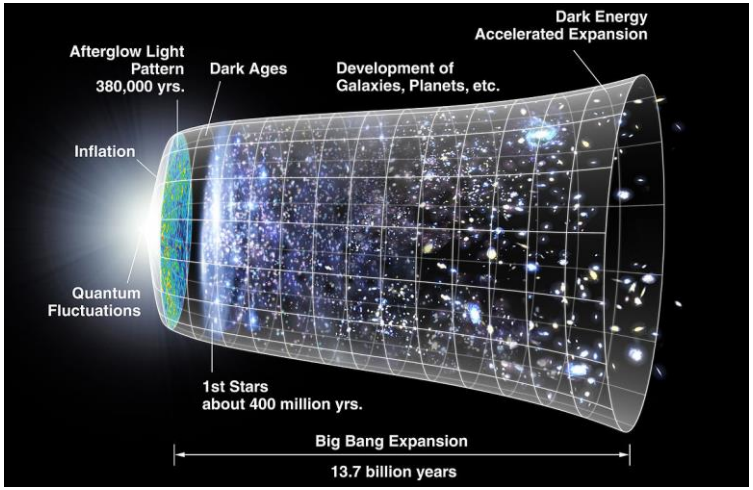

Gravitational waves from binary mergers

Distance can be measured directly from the gravitational wave signal!

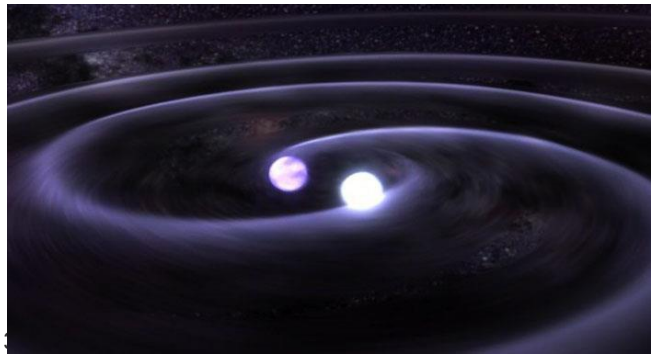

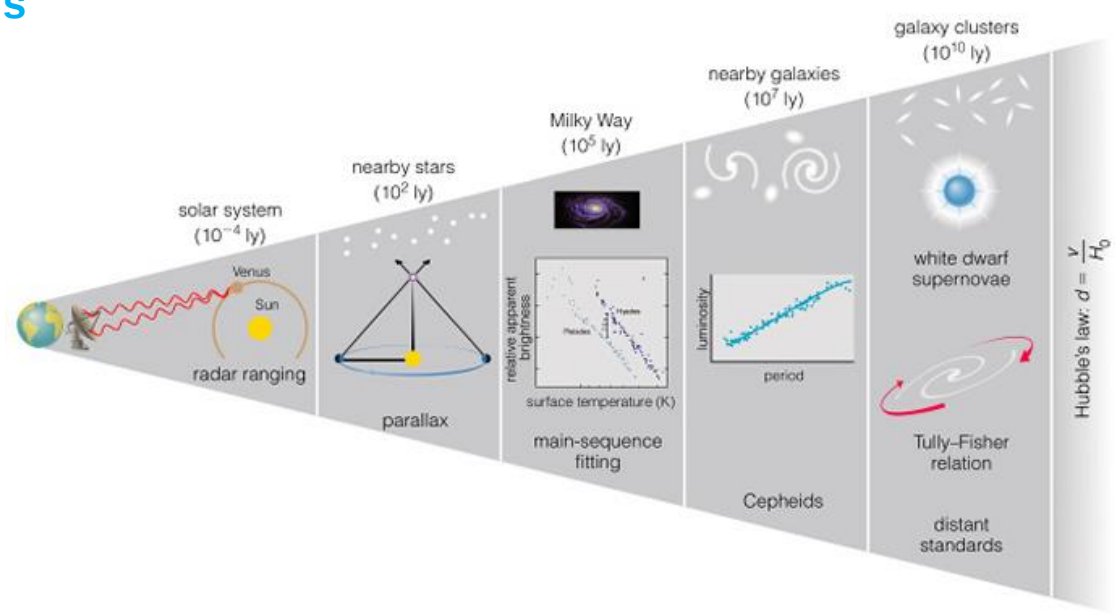

A new cosmic distance marker

A few tens of detections of binary neutron star mergers allow determining the Hubble parameters to about 1-2% accuracy

Measurement of the local expansion of the Universe

The Hubble constant

- Distance from GW signal
- Redshift from EM counterpart (galaxy NGC 4993)

LIGO+Virgo *et al*., Nature 551, 85 (2017)

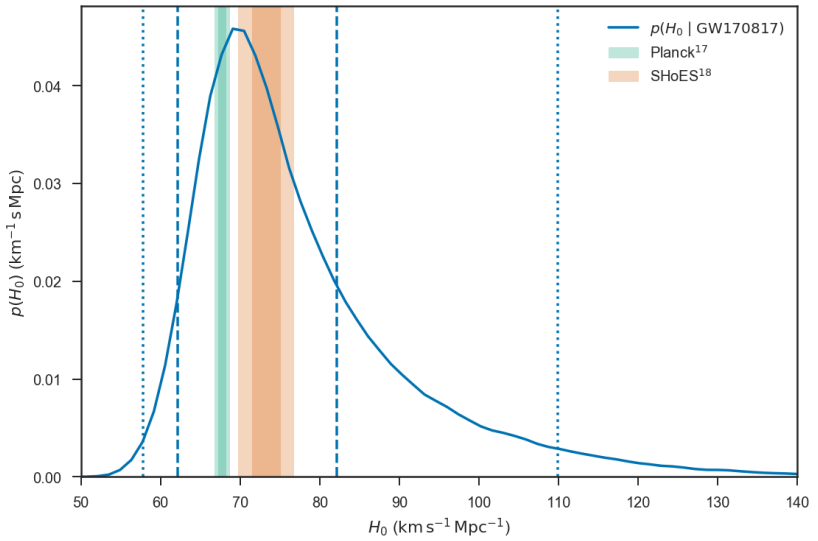

GW170817

- One detection: limited accuracy
- Few tens of detections with LIGO/Virgo will be needed to obtain O(1-2%) accuracy

Bernard Schutz, Nature 323, 310–311 (1986)

Walter Del Pozzo, PRD 86, 043011 (2012)

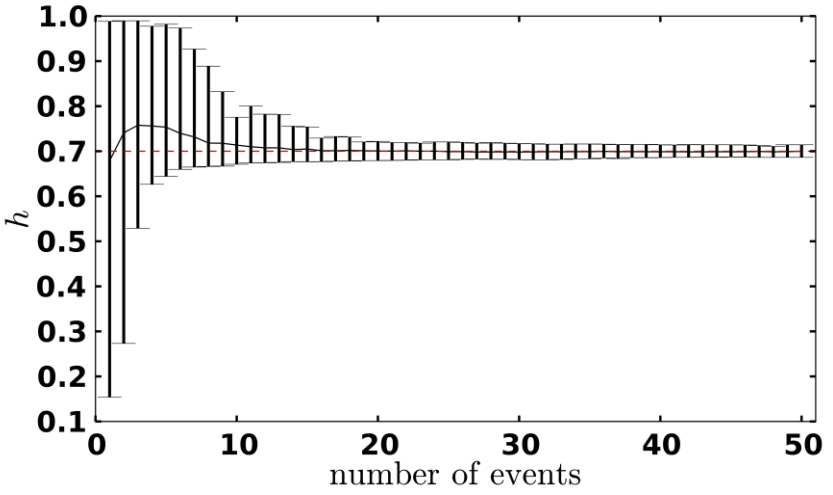

Third generation observatories allow studies of the Dark Energy equation of state parameter

Scientific impact of gravitational wave science

Multi-messenger astronomy started: a broad community is relying of detection of gravitational waves
Scientific program is limited by the sensitivity of LVC instruments over the entire frequency range

Fundamental physics

Access to dynamic strong field regime, new tests of General Relativity
Black hole science: inspiral, merger, ringdown, quasi-normal modes, echo's
Lorentz-invariance, equivalence principle, polarization, parity violation, axions

Astrophysics

First observation for binary neutron star merger, relation to sGRB
Evidence for a kilonova, explanation for creation of elements heavier than iron

Astronomy

Start of gravitational wave astronomy, population studies, formation of progenitors, remnant studies

Cosmology

Binary neutron stars can be used as standard “sirens”
Dark Matter and Dark Energy

Nuclear physics

Tidal interactions between neutron stars get imprinted on gravitational waves
Access to equation of state

April 1, 2019: LIGO and Virgo started Observation run O3

Joining O3 is another big step for Virgo

Virgo sensitivity: typically around 50 Mpc

Significant improvement (> 90%) with respect to the average sensitivity (26 Mpc) obtained in O2. We see a flat noise contribution at mid-frequencies, and significant 50 Hz noise. Power amounts to 18 W
Efficiency around 90%

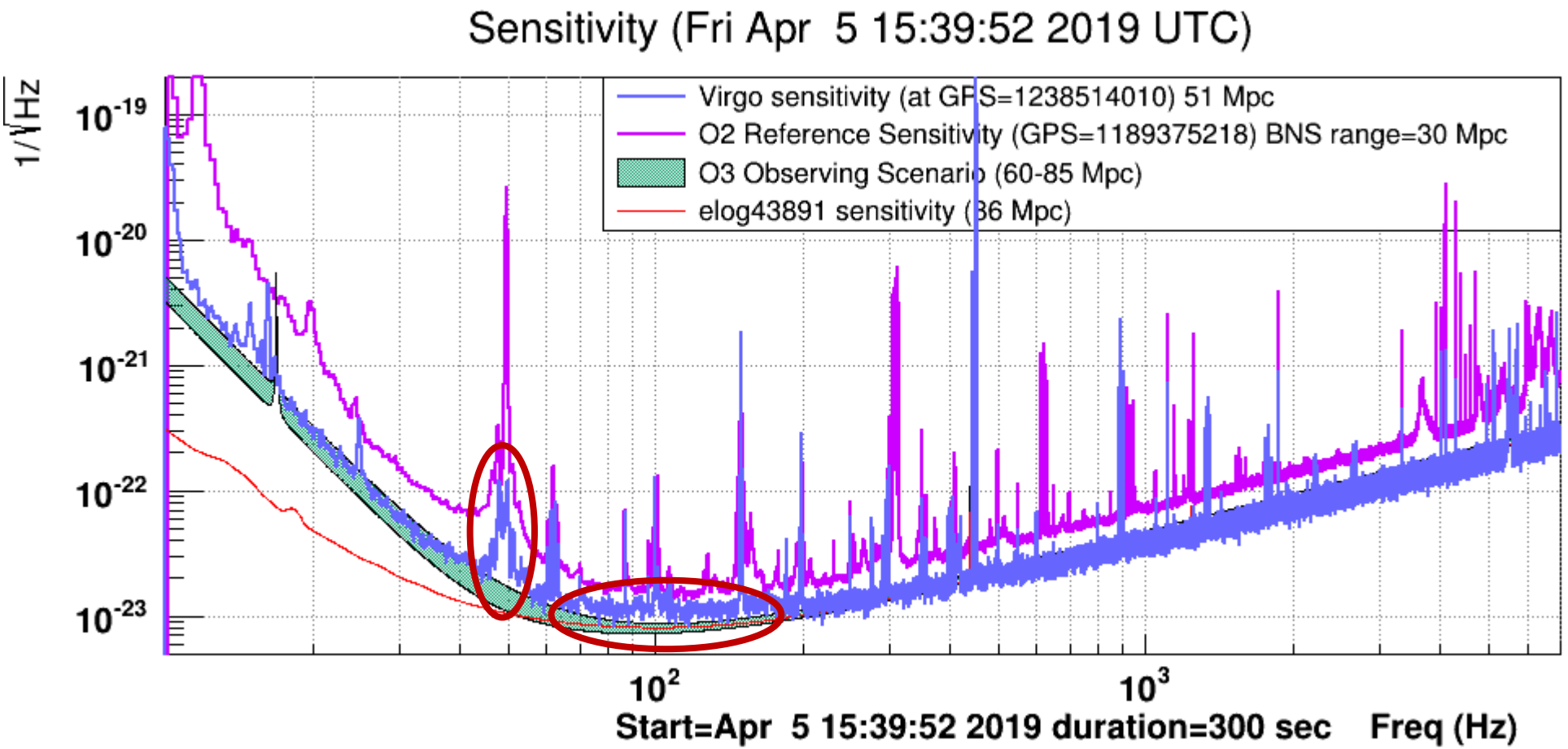

O3 is here! See https://gracedb.ligo.org/latest/

Public alerts in the 3rd science run: already more candidate events than O1 and O2 combined

Latest — as of 8 July 2019 09:03:46 UTC

Test and MDC events and superevents are not included in the search results by default; see the query help for information on how to search for events and superevents in those categories.

Query:

Search for: Superevent

Search

UID	Labels	t_start	t_0	t_end	FAR (Hz)	Created (UTC)
S190707q	ADVOK SKYMAP_READY EMBRIGHT_READY PASTRO_READY DQOK GCN_PRELIM_SENT	1246527223.118398	1246527224.181226	1246527225.284180	5.265e-12	2019-07-07 09:33:44 UTC
S190706ai	PE_READY ADVOK SKYMAP_READY EMBRIGHT_READY PASTRO_READY DQOK GCN_PRELIM_SENT	1246487218.321541	1246487219.344727	1246487220.585938	1.901e-09	2019-07-06 22:26:57 UTC
S190701ah	PE_READY ADVOK SKYMAP_READY EMBRIGHT_READY PASTRO_READY DQOK GCN_PRELIM_SENT	1246048403.576563	1246048404.577637	1246048405.814941	1.916e-08	2019-07-01 20:33:24 UTC
S190630ag	PE_READY ADVOK SKYMAP_READY EMBRIGHT_READY PASTRO_READY DQOK GCN_PRELIM_SENT	1245955942.175325	1245955943.179550	1245955944.183184	1.435e-13	2019-06-30 18:52:28 UTC
S190602aq	PE_READY ADVOK SKYMAP_READY EMBRIGHT_READY PASTRO_READY DQOK GCN_PRELIM_SENT	1243533584.081266	1243533585.089355	1243533586.346191	1.901e-09	2019-06-02 17:59:51 UTC
S190524q	ADVNO SKYMAP_READY EMBRIGHT_READY PASTRO_READY DQOK GCN_PRELIM_SENT	1242708743.678669	1242708744.678669	1242708746.133301	6.971e-09	2019-05-24 04:52:30 UTC
S190521r	PE_READY ADVOK SKYMAP_READY EMBRIGHT_READY PASTRO_READY DQOK GCN_PRELIM_SENT	1242459856.453418	1242459857.460739	1242459858.642090	3.168e-10	2019-05-21 07:44:22 UTC
S190521g	PE_READY ADVOK SKYMAP_READY EMBRIGHT_READY PASTRO_READY DQOK GCN_PRELIM_SENT	1242442966.447266	1242442967.606934	1242442968.888184	3.801e-09	2019-05-21 03:02:49 UTC
S190519bj	PE_READY ADVOK SKYMAP_READY EMBRIGHT_READY PASTRO_READY DQOK GCN_PRELIM_SENT	1242315361.378873	1242315362.655762	1242315363.676270	5.702e-09	2019-05-19 15:36:04 UTC
S190518bb	ADVNO SKYMAP_READY EMBRIGHT_READY PASTRO_READY DQOK GCN_PRELIM_SENT	1242242376.474609	1242242377.474609	1242242380.922655	1.004e-08	2019-05-18 19:19:39 UTC
S190517h	PE_READY ADVOK SKYMAP_READY EMBRIGHT_READY PASTRO_READY DQOK GCN_PRELIM_SENT	1242107478.819517	1242107479.994141	1242107480.994141	2.373e-09	2019-05-17 05:51:23 UTC
S190513bm	ADVOK SKYMAP_READY EMBRIGHT_READY PASTRO_READY DQOK GCN_PRELIM_SENT	1241816085.736106	1241816086.869141	1241816087.869141	3.734e-13	2019-05-13 20:54:48 UTC
S190512at	PE_READY ADVOK SKYMAP_READY EMBRIGHT_READY PASTRO_READY DQOK GCN_PRELIM_SENT	1241719651.411441	1241719652.416286	1241719653.518066	1.901e-09	2019-05-12 18:07:42 UTC
S190510g	ADVOK SKYMAP_READY EMBRIGHT_READY PASTRO_READY DQOK GCN_PRELIM_SENT	1241492396.291636	1241492397.291636	1241492398.293185	8.834e-09	2019-05-10 03:00:03 UTC
S190503bf	ADVOK SKYMAP_READY EMBRIGHT_READY PASTRO_READY DQOK GCN_PRELIM_SENT	1240944861.288574	1240944862.412598	1240944863.422852	1.636e-09	2019-05-03 18:54:26 UTC
S190426c	PE_READY ADVOK SKYMAP_READY EMBRIGHT_READY PASTRO_READY DQOK GCN_PRELIM_SENT	1240327332.331668	1240327333.348145	1240327334.353516	1.947e-08	2019-04-26 15:22:15 UTC
S190425z	ADVOK SKYMAP_READY EMBRIGHT_READY PASTRO_READY DQOK	1240215502.011549	1240215503.011549	1240215504.018242	4.538e-13	2019-04-25 08:18:26 UTC
S190421ar	PE_READY ADVOK SKYMAP_READY EMBRIGHT_READY PASTRO_READY DQOK GCN_PRELIM_SENT	1239917953.250977	1239917954.409180	1239917955.409180	1.489e-08	2019-04-21 21:39:16 UTC
S190412m	PE_READY ADVOK SKYMAP_READY EMBRIGHT_READY PASTRO_READY DQOK GCN_PRELIM_SENT	1239082261.146717	1239082262.222168	1239082263.229492	1.683e-27	2019-04-12 05:31:03 UTC
S190408an	PE_READY ADVOK SKYMAP_READY EMBRIGHT_READY PASTRO_READY DQOK GCN_PRELIM_SENT	1238782699.268296	1238782700.287958	1238782701.359863	2.811e-18	2019-04-08 18:18:27 UTC
S190405ar	ADVNO SKYMAP_READY EMBRIGHT_READY PASTRO_READY DQOK	1238515307.863646	1238515308.863646	1238515309.863646	2.141e-04	2019-04-05 16:01:56 UTC

LIGO VIRGO LSC

Virgo's low latency computing is working as designed. Automatic public alerts not so "automatic" (yet)

Three events were retracted by the LVC after more detailed analysis

A new **binary neutron star** event: only LIGO Livingston and Virgo were operational, thus large uncertainty in sky position. A **neutron star-black hole** event: LIGO Livingston, LIGO Hanford, and Virgo operational, but no EM counterpart found

https://en.wikipedia.org/wiki/List_of_gravitational_wave_observations

Public alerts in the 3rd science run: already more candidate events than O1 and O2 combined

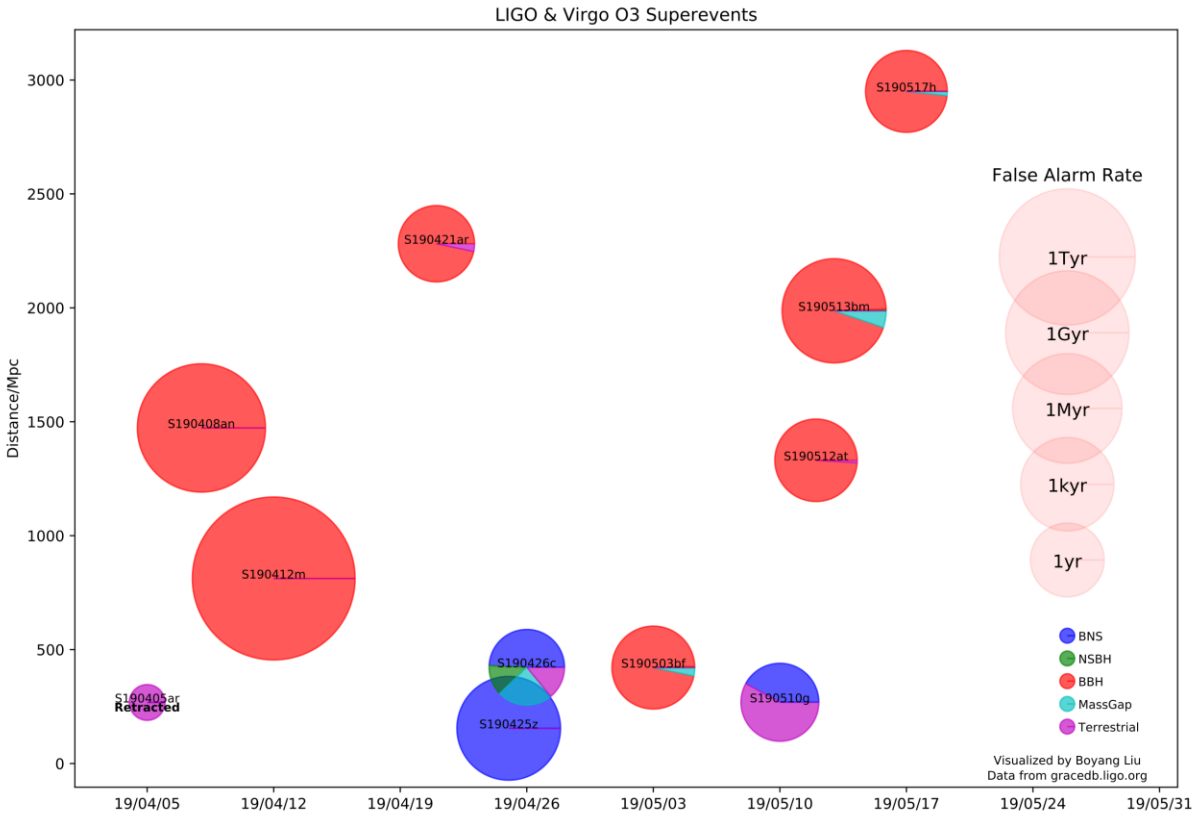

Virgo's low latency computing is working as designed. Automatic public alerts not so "automatic" (yet)

Three events were retracted by the LVC after more detailed analysis

A new **binary neutron star** event: only LIGO Livingston and Virgo were operational, thus large uncertainty in sky position. A **neutron star-black hole** event: LIGO Livingston, LIGO Hanford, and Virgo operational, but no EM counterpart found

The path forward …

AdV+ as the next incremental step forward in sensitivity

AdV+ is the plan to maximize Virgo's sensitivity within the constrains of the EGO site. It has the potential to increase Virgo's detection rate by up to an order of magnitude

AdV+ features

Maximize science

Secure Virgo's scientific relevance

Safeguard investments by scientists and funding agencies

Implement new innovative technologies

De-risk technologies needed for third generation observatories

Attractive for groups wanting to enter the field

Upgrade activities

Tuned signal recycling and HPL: 120 Mpc

Frequency dependent squeezing: 150 Mpc

Newtonian noise cancellation: 160 Mpc

Larger mirrors (105 kg): 200-230 Mpc

Improved coatings: 260-300 Mpc

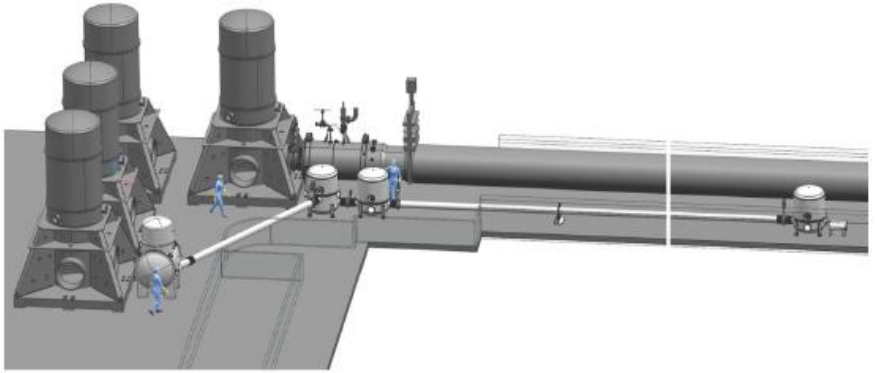

Virgo will implemented signal recycling after O3

Signal recycling will improve Virgo's sensitivity at medium to high frequency

Virgo's strain sensitivity

- Effect of no signal recycling is apparent. Also injected laser power 18 W, no squeezing, 3 km, …

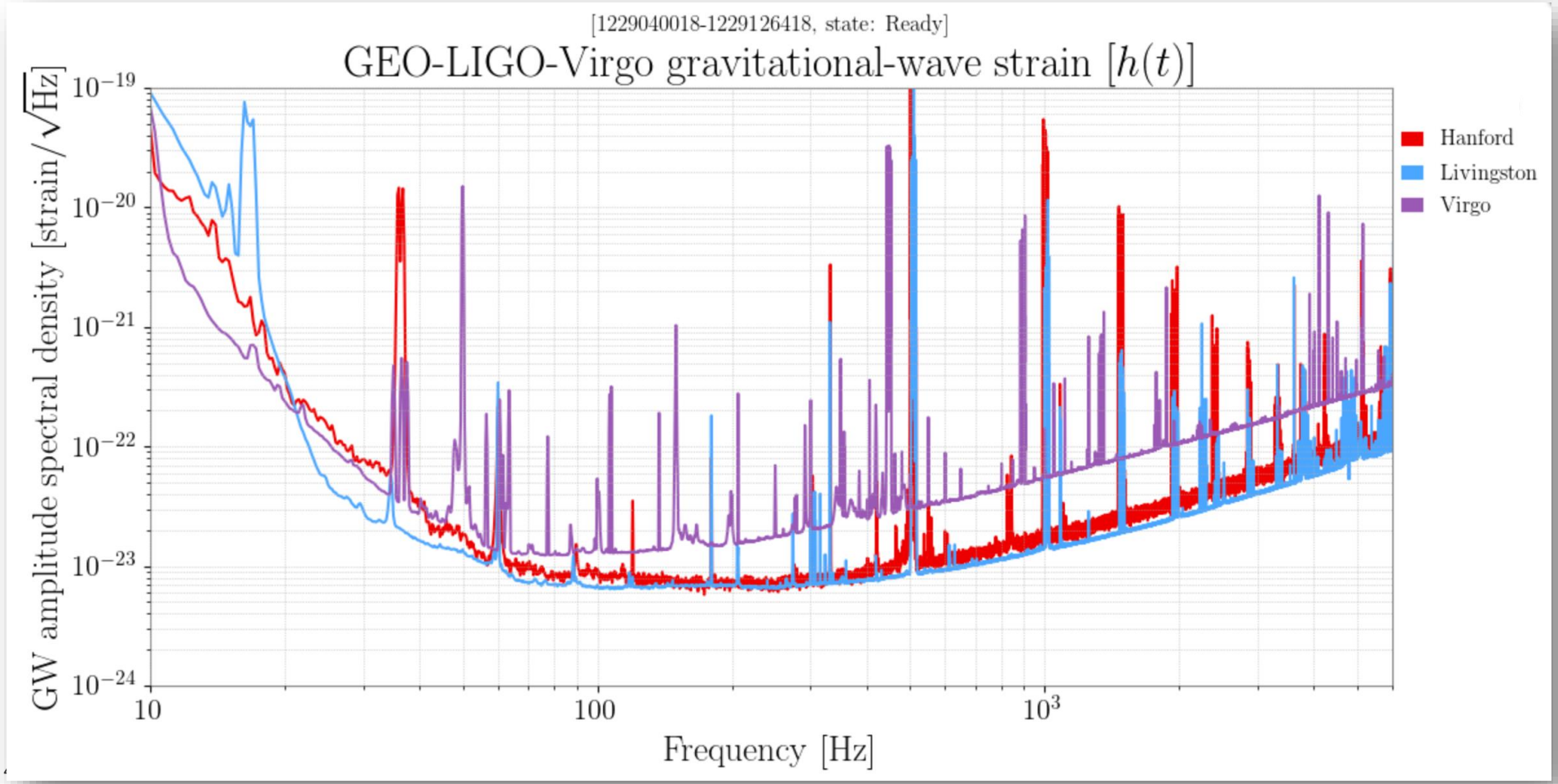

Frequency dependent squeezing

Most important part of the AdV+ upgrade project

Nikhef contributes to

a) Optical system design
b) High-finesse 300 m long filter cavity
c) Vibration isolation of in-vacuum squeezer bench and beam matching microtowers

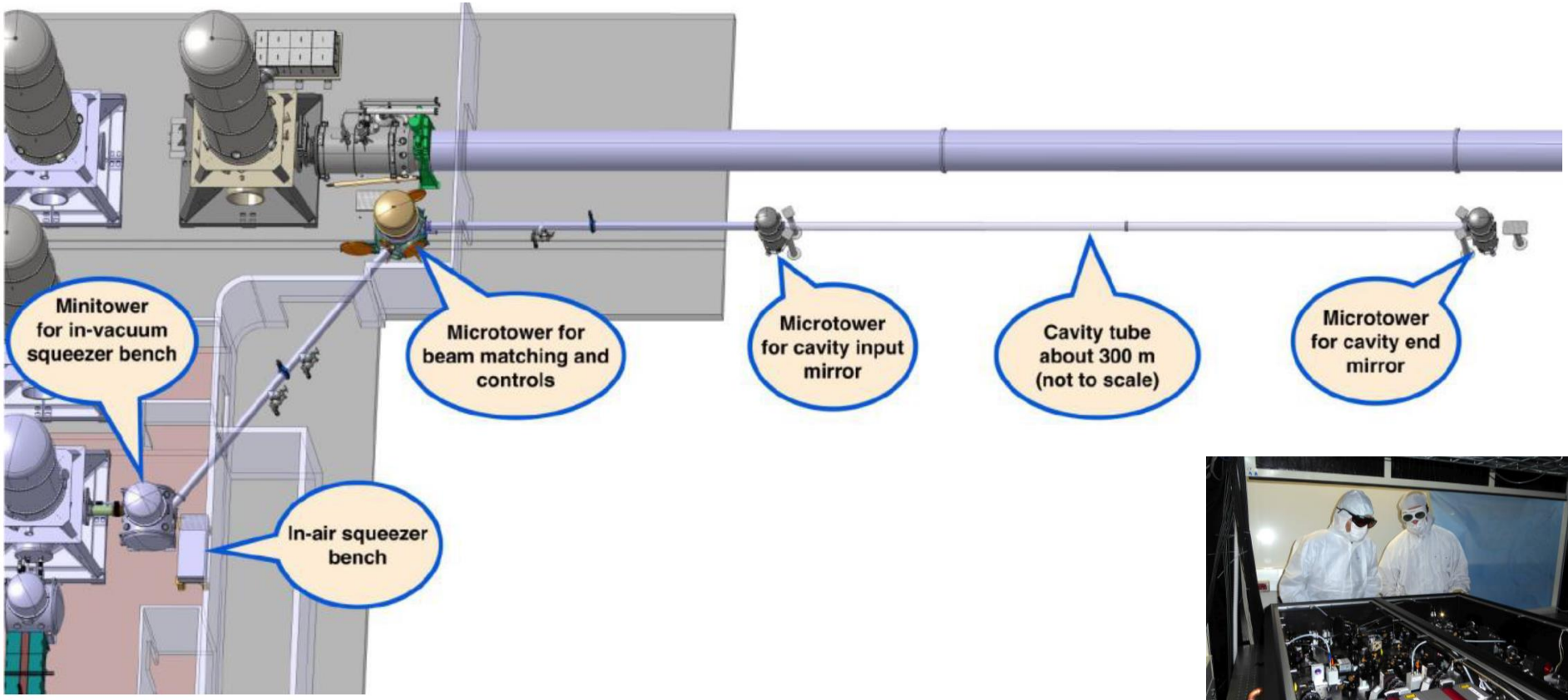

Virgo squeezer from AEI Hannover

Phase 1: reaching the thermal noise wall

Increase laser power, implement signal recycling, frequency dependent squeezing and Newtonian noise suppression

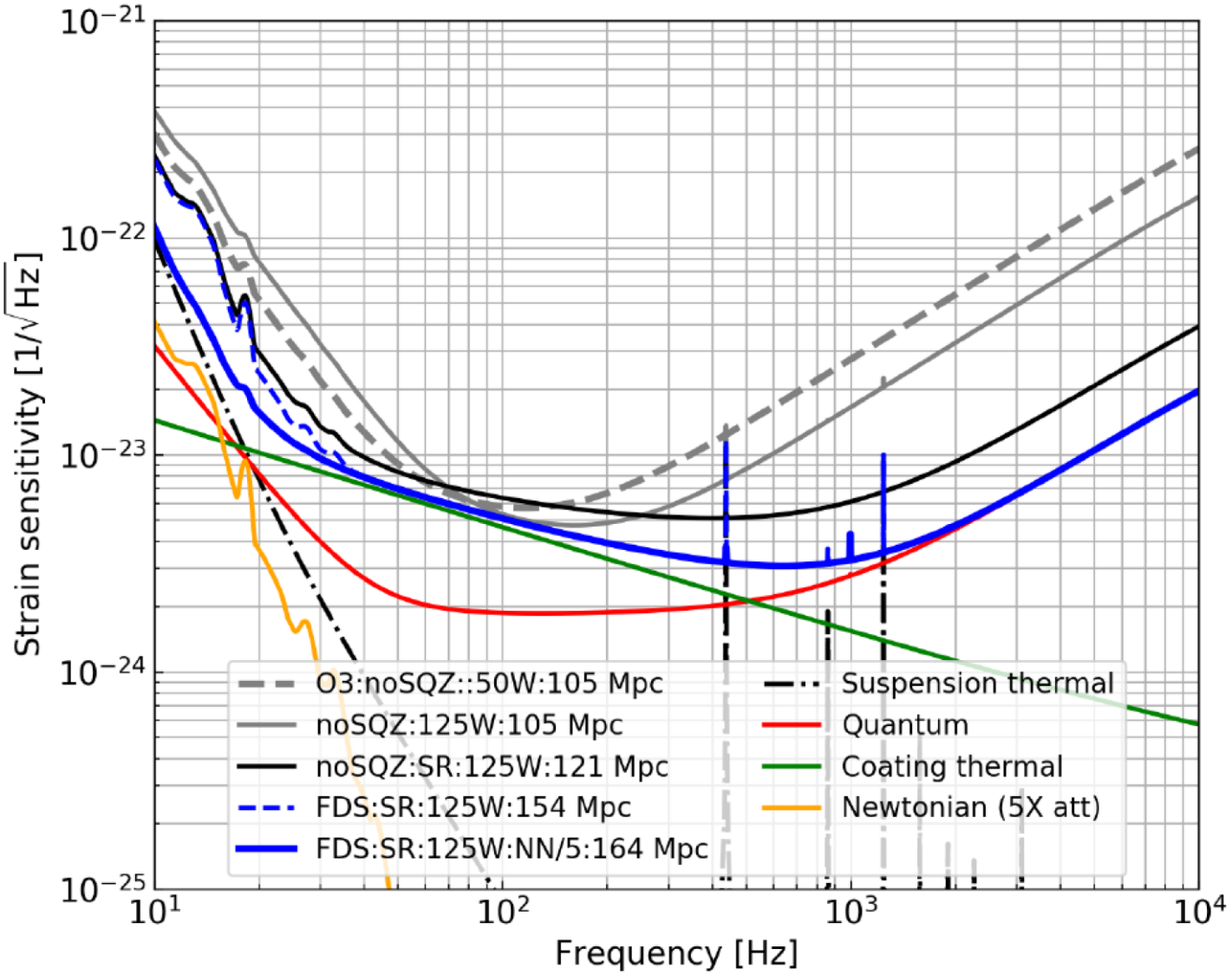

Phase 2: pushing the thermal noise wall down

Implement larger ETMs and employ better coatings

Even better sensitivity can be obtained by replacing all mirrors, but this would be too invasive

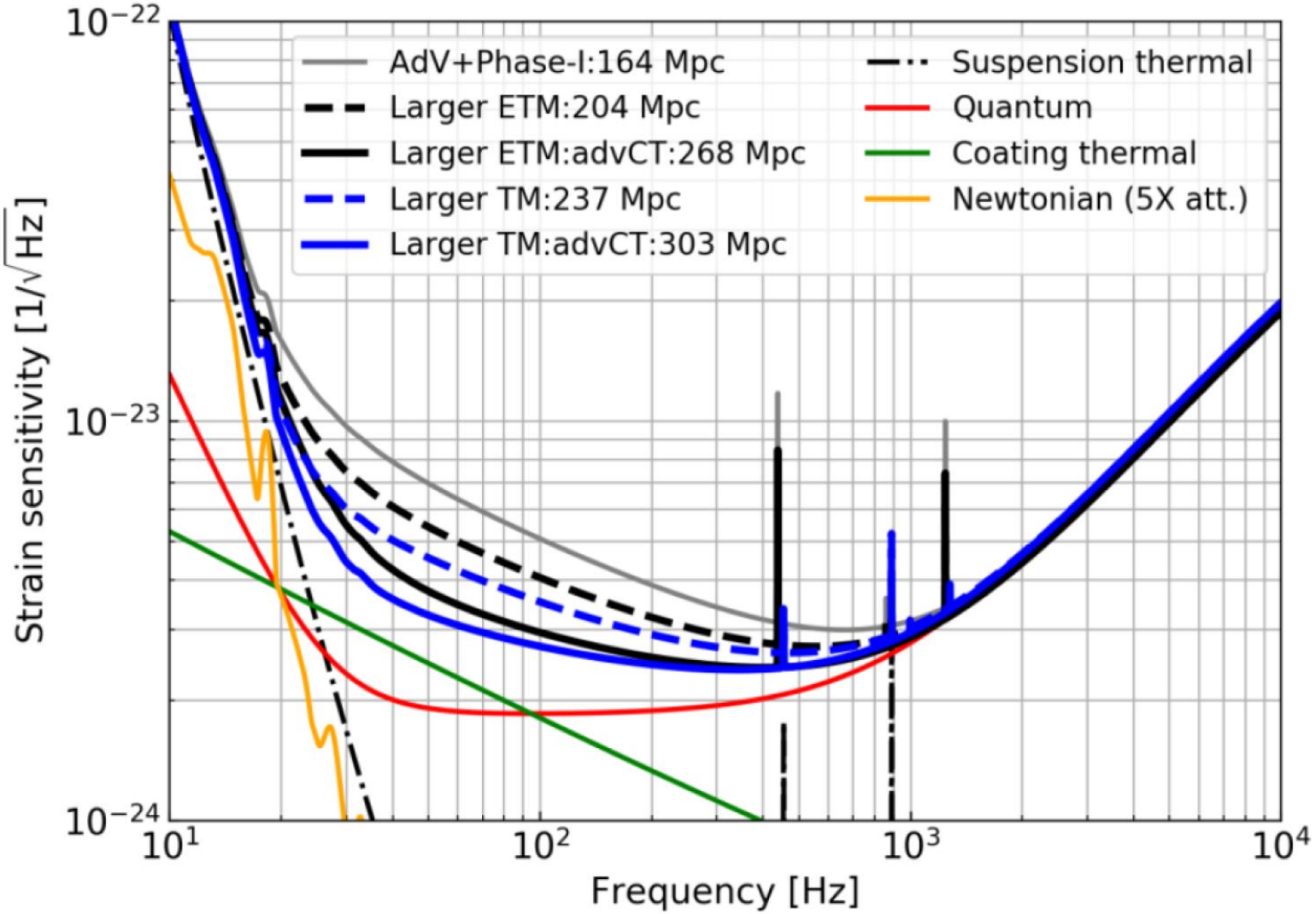

AdV+ upgrade and extreme mirror technology

Laboratoire des Matériaux Avancés LMA at Lyon produced the coatings used on the main mirrors of the two working gravitational wave detectors: Advanced LIGO and Virgo. These coatings feature low losses, low absorption, and low scattering properties

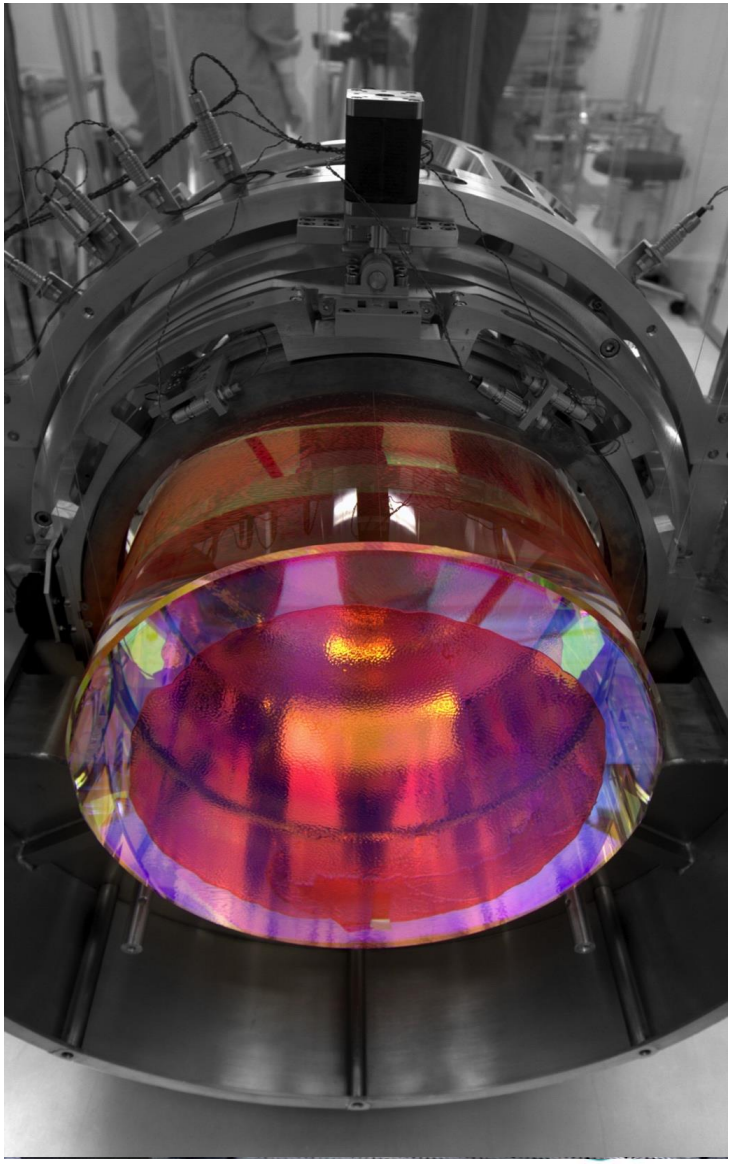

Features

- Flatness < 0.5 nm rms over central 160 mm of mirrors by using ion beam polishing (robotic silica deposition was investigated)
- Ti:Ta_2O_5 and SiO_2 stacks with optical absorption about 0.3 ppm

Expand LMA capabilities for next generation

LMA is the only coating group known to be capable of scaling up

Scheduling of science runs, AdV+ installation and commissioning

Five year plan for observational runs, commissioning and upgrades

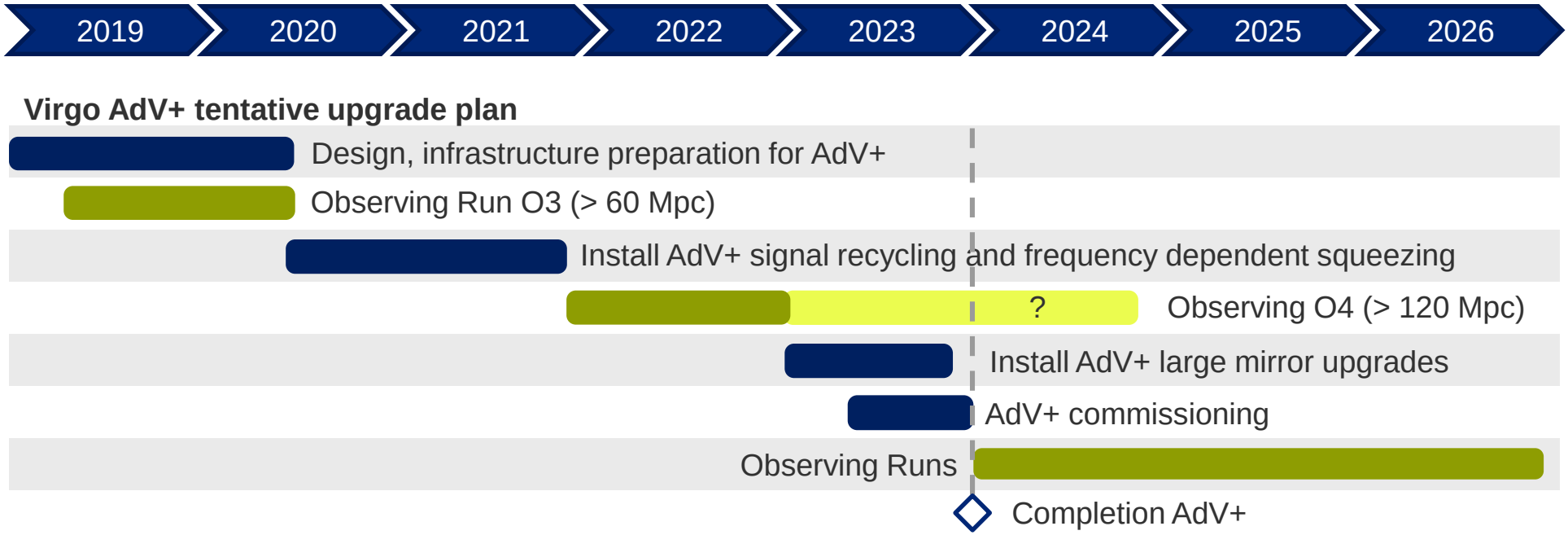

Commissioning break in October 2019

Duration of O3: until the end of April 2020 (duration of O4 has not been decided)

Break between O3 and O4 probably around 18 months (allow installation and commissioning)

AdV+ to be carried out in parallel with LIGO's A+ upgrade

AdV+ is part of a strategy to go from 2nd generation to Einstein Telescope

Einstein Telescope and Cosmic Explorer

Realizing the next gravitational wave observatories is a coordinated effort with US to create a worldwide 3G network

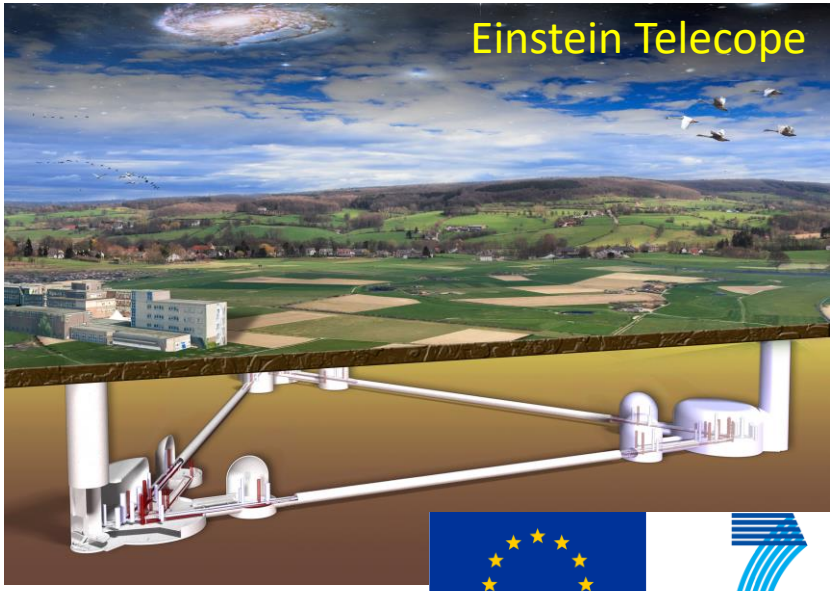

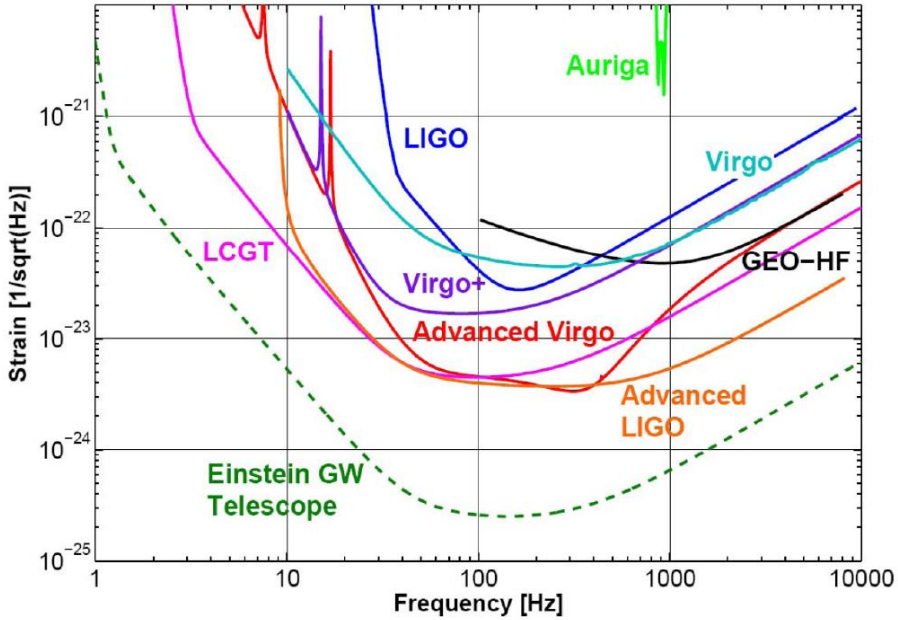

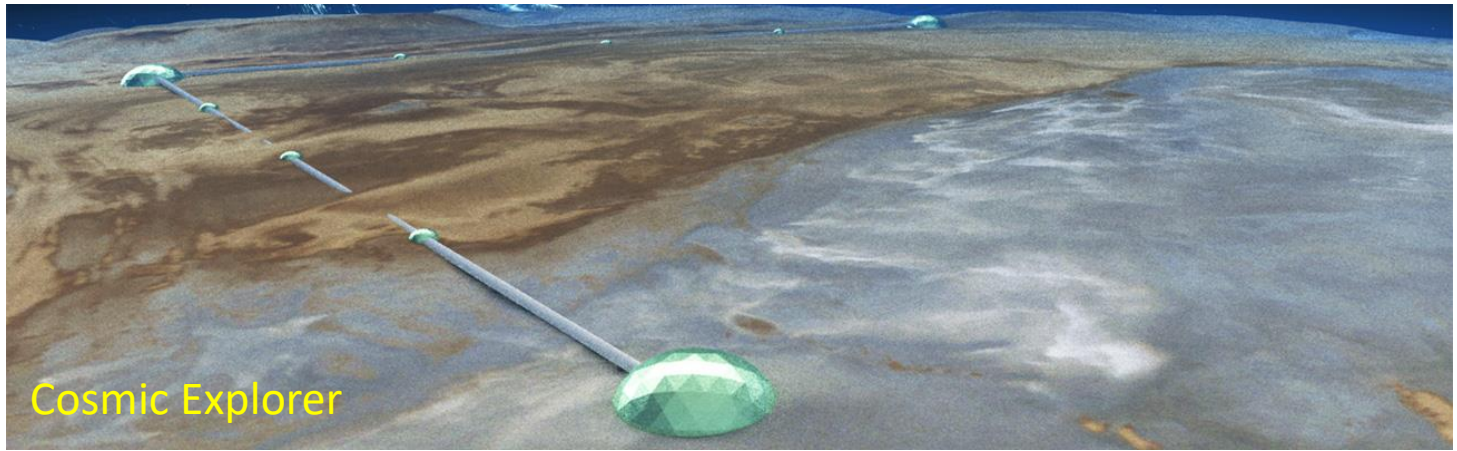

Einstein Telescope and Cosmic Explorer

Einstein Telescope will feature excellent low-frequency sensitivity and have great discovery potential

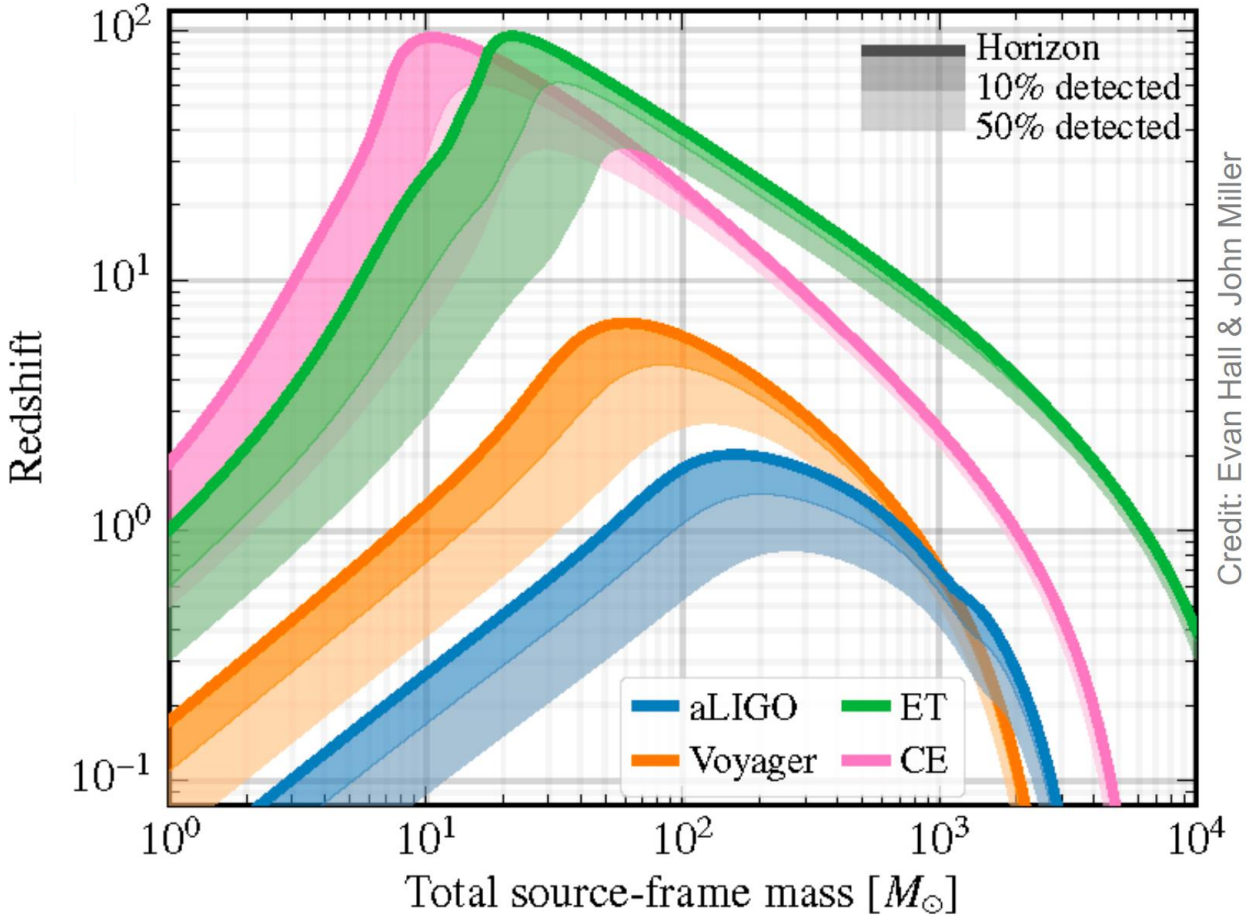

For science case, see https://www.dropbox.com/s/gihpzcue4qd92dt/science-case.pdf?dl=0

Einstein Telescope

Einstein Telescope can observe BBH mergers to red shifts of about 100. This allows a new approach to cosmography. Study primordial black holes, BH from population III stars (first metal producers), *etc*.

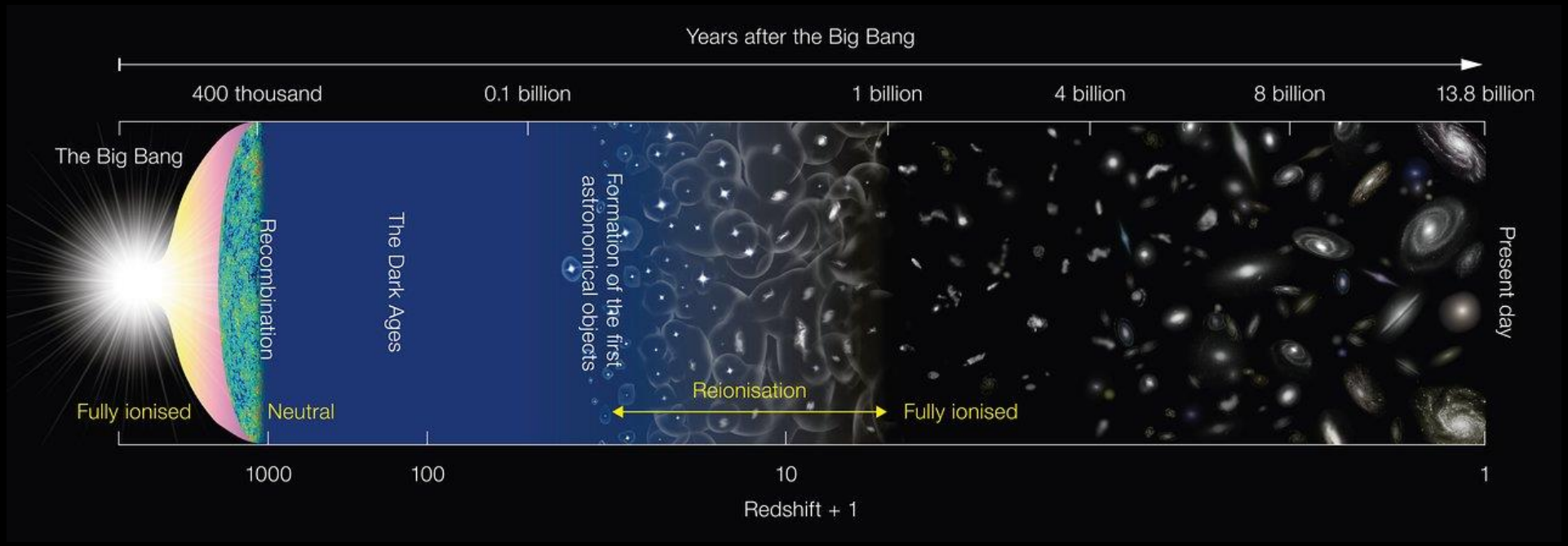

Einstein Telescope has direct access to signals from black hole mergers in this range

Bright future for gravitational wave research

LIGO and Virgo are operational. KAGRA in Japan joins this year, LIGO-India under construction. ESA launches LISA in 2034. Einstein Telescope and CE CDRs financed. Strong support by APPEC

Gravitational wave research

- LIGO and Virgo operational
- KAGRA to join this year
- LIGO-India under construction (2025)
- ESA selects LISA, NASA rejoins
- Pulsar Timing Arrays, such as EPTA and SKA
- Cosmic Microwave Background radiation

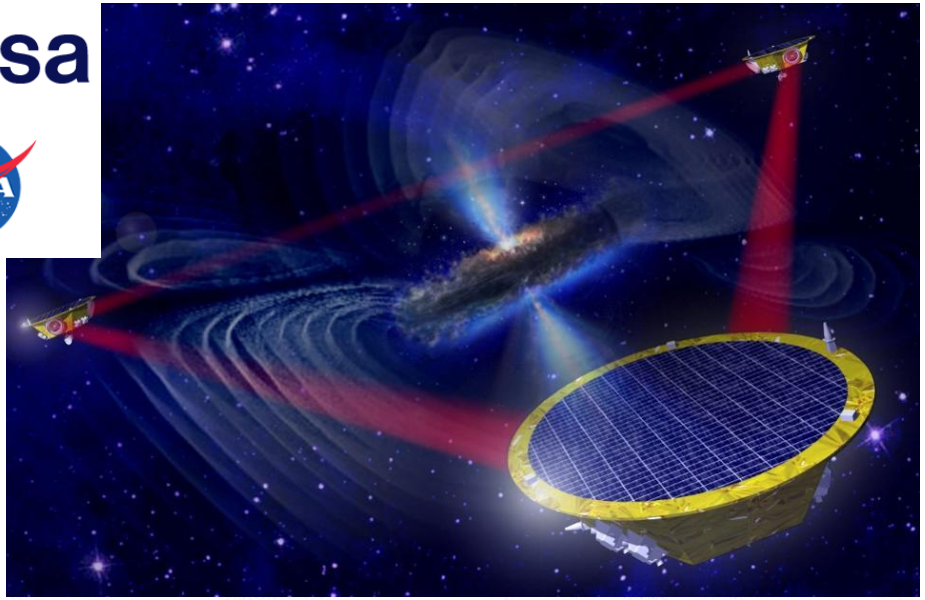

Einstein Telescope and Cosmic Explorer

- CDR ET financed by EU in FP7, CE by NSF
- APPEC gives GW a prominent place in the new Roadmap and especially the realization of ET

Next steps for 3G

- Organize the community and prepare a credible plan for EU funding agencies
- ESFRI Roadmap (2020)
- Support 3G: http://www.et-gw.eu/index.php/letter-of-intent

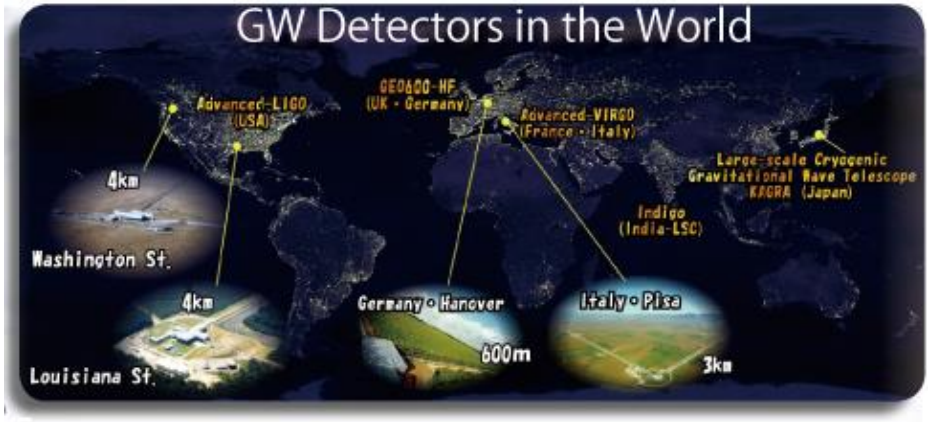

3G science

Detailed studies of gravity, near black holes. Early warning to EM follow-up community. Precision tests of detailed aspects of CBC. Cross correlation of the largest data sets. Access to early Universe

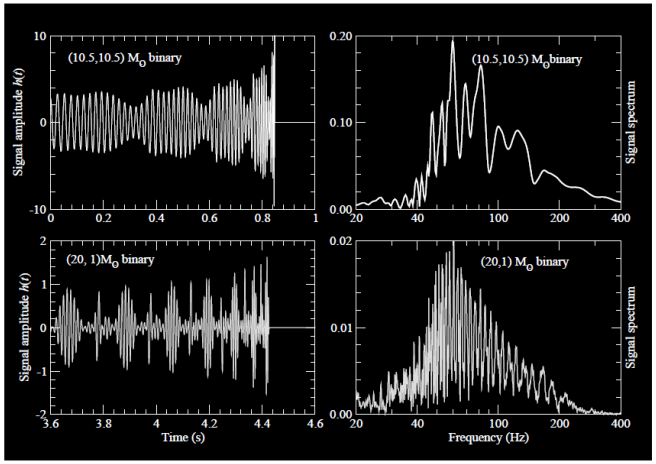

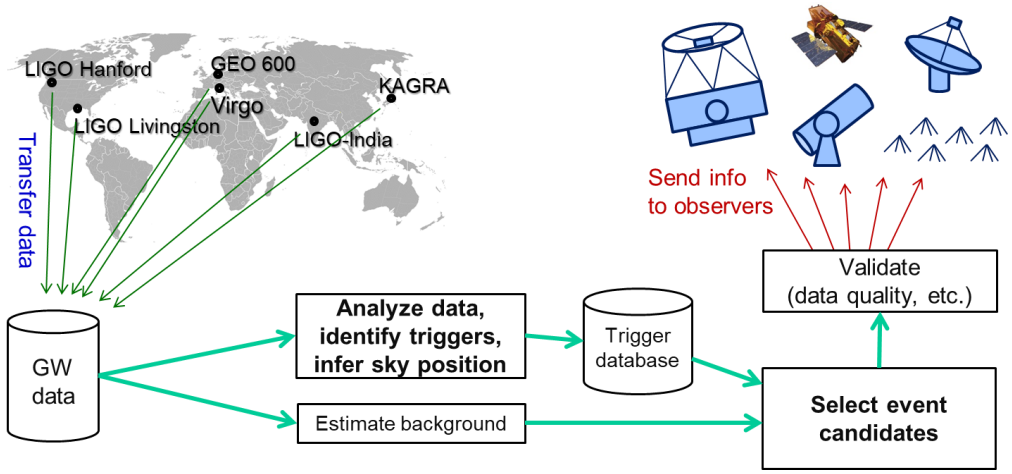

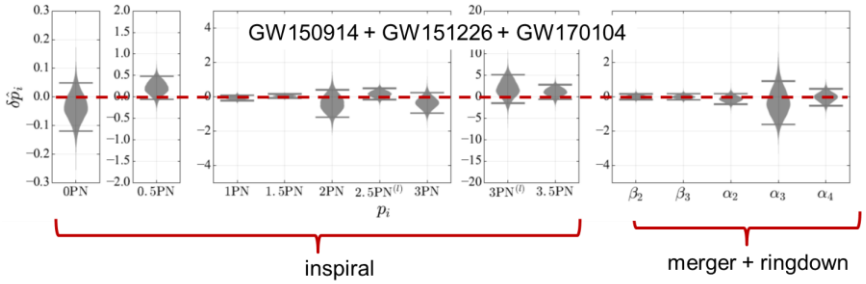

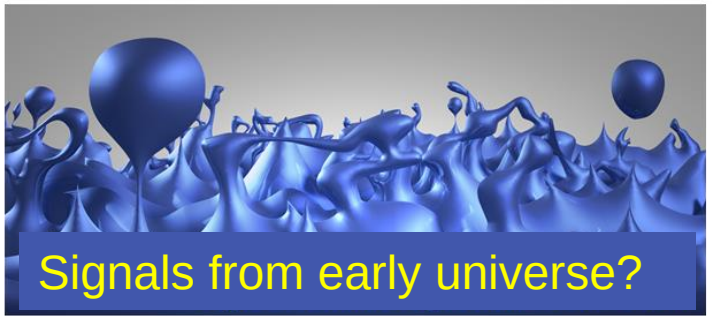

Multi-messenger astronomy

THESEUS: a key space mission for Multi-Messenger Astrophysics

G. Stratta, R. Ciolfi, L. Amati, G. Ghirlanda, N. Tanvir, E. Bozzo, D. Gotz, P. O'Brien, F. Frontera, J. P. Osborne, L. Rezzolla, A. Rossi, E. Maiorano, S. Vinciguerra, C. Guidorzi, A. Drago, L. Nicastro, E. Palazzi, M. Branchesi, M. Boer, E. Brocato, A. Bulgarelli, S. Covino, V. D'Elia, M. G. Dainotti, M. De Pasquale, B. Gendre, P. Jonker, F. Longo, S. Mereghetti, R. Mignani, C. G. Mundell, S. Piranomonte, M. Razzano, D. Szécsi, M. van Putten, B. Zhang, R. Hudec, S. Vergani, D. Malesani, P. D'Avanzo, S. Colafrancesco, A. Stamerra, J. Caruana, R. Starling, R. Willingale, R. Salvaterra, U. Maio, J. Greiner, P. Rosati, C. Labanti, F. Fuschino, R. Campana, A. Grado, M. Colpi, T. Rodic, B. Patricelli, M. Bernardini

arXiv:1712.08153

December 2017
Advances in Space Research
DOI: 10.1016/j.asr.2018.04.013

We will update this figure